



**HAL**  
open science

## Further characterisation of late somatosensory evoked potentials using electroencephalogram and magnetoencephalogram source imaging

Sahar Hssain-Khalladi, Alain Giron, Clément Huneau, Christophe Gitton, Denis Schwartz, Nathalie George, Michel Le van Quyen, Guillaume Marrelec, Veronique Marchand-Pauvert

### ► To cite this version:

Sahar Hssain-Khalladi, Alain Giron, Clément Huneau, Christophe Gitton, Denis Schwartz, et al.. Further characterisation of late somatosensory evoked potentials using electroencephalogram and magnetoencephalogram source imaging. *European Journal of Neuroscience*, 2024, 60 (1), pp.3772-3794. 10.1111/ejn.16379 . hal-04556794v2

**HAL Id: hal-04556794**

<https://hal.sorbonne-universite.fr/hal-04556794v2>

Submitted on 5 Jul 2024


**HAL** is a multi-disciplinary open access archive for the deposit and dissemination of scientific research documents, whether they are published or not. The documents may come from teaching and research institutions in France or abroad, or from public or private research centers.

L'archive ouverte pluridisciplinaire **HAL**, est destinée au dépôt et à la diffusion de documents scientifiques de niveau recherche, publiés ou non, émanant des établissements d'enseignement et de recherche français ou étrangers, des laboratoires publics ou privés.



Distributed under a Creative Commons Attribution - NonCommercial - NoDerivatives 4.0 International License

# Further characterisation of late somatosensory evoked potentials using electroencephalogram and magnetoencephalogram source imaging

Sahar Hssain-Khalladi<sup>1,2</sup> | Alain Giron<sup>1</sup> | Clément Huneau<sup>3</sup> |  
 Christophe Gitton<sup>4</sup> | Denis Schwartz<sup>4</sup> | Nathalie George<sup>4</sup> |  
 Michel Le Van Quyen<sup>1</sup> | Guillaume Marrelec<sup>1</sup> | Véronique Marchand-Pauvert<sup>1</sup> 

<sup>1</sup>Sorbonne Université, Inserm, CNRS, Laboratoire d'Imagerie Biomédicale, LIB, Paris, France

<sup>2</sup>Sorbonne Université, Laboratoire d'Excellence SMART, Paris, France

<sup>3</sup>Université de Nantes, CNRS, Laboratoire des Sciences du Numérique de Nantes, LS2N, Nantes, France

<sup>4</sup>Sorbonne Université, Inserm, CNRS, Institut du Cerveau, ICM, Paris, France

## Correspondence

Véronique Marchand-Pauvert,  
 Laboratoire d'Imagerie Biomédicale (LIB),  
 Campus des Cordeliers, Bât. A, 3<sup>e</sup> étage,  
 15 rue de l'École de Médecine, Paris  
 75006, France.  
 Email: [veronique.marchand@upmc.fr](mailto:veronique.marchand@upmc.fr)

## Funding information

Agence Nationale de la Recherche (ANR),  
 Grant/Award Number: ANR-11-IDEX-  
 0004-02; Inserm; Sorbonne Université;  
 CNRS

Edited by: Christoph M. Michel

## Abstract

Beside the well-documented involvement of secondary somatosensory area, the cortical network underlying late somatosensory evoked potentials (P60/N60 and P100/N100) is still unknown. Electroencephalogram and magnetoencephalogram source imaging were performed to further investigate the origin of the brain cortical areas involved in late somatosensory evoked potentials, using sensory inputs of different strengths and by testing the correlation between cortical sources. Simultaneous high-density electroencephalograms and magnetoencephalograms were performed in 19 participants, and electrical stimulation was applied to the median nerve (wrist level) at intensity between 1.5 and 9 times the perceptual threshold. Source imaging was undertaken to map the stimulus-induced brain cortical activity according to each individual brain magnetic resonance imaging, during three windows of analysis covering early and late somatosensory evoked potentials. Results for P60/N60 and P100/N100 were compared with those for P20/N20 (early response). According to literature, maximal activity during P20/N20 was found in central sulcus contralateral to stimulation site. During P60/N60 and P100/N100, activity was

**List of Abbreviations:** ECG, electrocardiogram; EEG, electroencephalogram; EOG, electrooculogram; I/O, input–output ratio; iPPC, inferior posterior parietal cortex; ISI, interstimulus interval; M1, primary motor cortex; MEG, magnetoencephalogram; MRI, magnetic resonance imaging; MT, motor threshold; PCC, posterior cingulate cortex; PM, premotor cortex; PT, perceptual threshold; ROIs, regions of interest; SEP, somatosensory evoked potentials; SI, primary somatosensory area; SII, secondary somatosensory area; SMA, supplemental motor area; SMG, supramarginal area; sPPC, superior posterior parietal cortex; STS, superior temporal sulcus.

Guillaume Marrelec and Véronique Marchand-Pauvert are co-last authors.

This is an open access article under the terms of the [Creative Commons Attribution-NonCommercial-NoDerivs](https://creativecommons.org/licenses/by-nc-nd/4.0/) License, which permits use and distribution in any medium, provided the original work is properly cited, the use is non-commercial and no modifications or adaptations are made.

© 2024 The Authors. *European Journal of Neuroscience* published by Federation of European Neuroscience Societies and John Wiley & Sons Ltd.

observed in contralateral primary sensorimotor area, secondary somatosensory area (on both hemispheres) and premotor and multisensory associative cortices. Late responses exhibited similar characteristics but different from P20/N20, and no significant correlation was found between early and late generated activities. Specific clusters of cortical activities were activated with specific input/output relationships underlying early and late somatosensory evoked potentials. Cortical networks, partly common to and distinct from early somatosensory responses, contribute to late responses, all participating in the complex somatosensory brain processing.

#### KEYWORDS

brain mapping, EEG, humans, MEG, somatosensory evoked potentials, source imaging

## 1 | INTRODUCTION

Somatosensory evoked potentials (SEPs) are investigated in clinics to evaluate the integrity of the peripheral and central sensory pathways. In clinical routine, sensory inputs are produced by stimulating peripheral nerves electrically, and the resulting cortical responses are most often collected with small single-use needles inserted in the scalp, at the C3/C4 standard electroencephalogram (EEG) locations, that is, over the primary sensorimotor cortex, contralateral and ipsilateral to the stimulation site. The reference electrode is extra-cephalic, most often using a pregelled surface electrode stuck on one ear lobe. The signals from the contralateral and ipsilateral cortices are then subtracted from each other, to evaluate the amplitude of the first biphasic response, that is, N20–P25 component (Morizot-Koutlidis et al., 2015). In line with the clinical use of SEPs, most of the researches focussed on the early components of cortical SEPs, with latency <35 ms (Passmore et al., 2014); the late components (>35 ms) have been investigated to a much lesser extent. In a previous study, we reported that the late SEPs (P60/N60 and P100/N100) are more depressed in patients with amyotrophic lateral sclerosis (ALS), compared with earlier components (P20/N20, P25/N25 and P30/N30), and we did not find any correlation between the early and late components (Sangari et al., 2016). Despite existing literature, questions remain on the precise origin and characteristics of late components (source locations and sensitivity to peripheral inputs) and interaction with earlier components, to evaluate the altered cortical excitability in patients with ALS.

Based on dipole localisation from scalp, epidural and intracranial EEG, it has been well established that P20/N20 is generated in the primary somatosensory area (SI) and that the following peaks, P25/N25 and P30/N30, are likely due to activity in posterior parietal, motor and

premotor areas (Allison et al., 1991; Mauguire, 2005; Passmore et al., 2014). Much less is known on later components with latency >40 ms, but it has been admitted that the secondary somatosensory cortex (SII) might be particularly involved in P60/N60 and P100/N100 and, to a lesser extent in earlier responses, with latency <40 ms (Allison et al., 1991; Mauguire, 2005; Passmore et al., 2014). Several methods of source imaging, based on the resolution of inverse problem, have been developed using magnetoencephalography (MEG) and EEG (for references, see Baillet, 2017; Michel & He, 2019). Their first applications to SEPs gave rise to consistent results with previous studies using dipole localisation, regarding the origin of P20/N20 in SI and the area 3b in particular (Allison et al., 1991; Buchner et al., 1994; Nakamura et al., 1998). Later, P20/N20 was used to develop new methods of source imaging, to compare their abilities to localise the dipole in SI and to test the influence of stimulation type, head modelling and the use of combined or separate MEG/EEG recordings (Antonakakis et al., 2019; Huang et al., 2007; Komssi et al., 2004; Mideksa et al., 2012; Rezaei et al., 2021). However, to date, the cortical activation map after peripheral nerve stimulation and its temporality has not been studied in detail. Specifically, there is no detailed report of source location (except SII) during late components while this would help to deepen the knowledge on the origin of the late cortical responses to peripheral nerve stimulation (cortical map of induced activity and interaction between early and late components and between cortical areas involved).

Previous studies have explored the influence of stimulation intensity on the early and late components and on the responses of SI or SII areas, assuming that if the input/output (I/O) relationships are different between early and late components or between SI and SII cortical areas, the underlying neural encoding is different and likely plays a different role in the somatosensory brain

processing (Gerber & Meinck, 2000; Huttunen, 1995; Jousmäki & Forss, 1998; Lin et al., 2003; Onishi et al., 2013; Torquati et al., 2002). Globally, all these studies revealed that the somatosensory evoked cortical responses increased with sensory afferent inputs. Regarding the intensity of electrical stimulus, the size of the dipoles increased with stimulus strength before they plateaued at intensity around the motor threshold (MT) (one times the MT; threshold intensity for activating the motor axons in the peripheral nerve). There was a trend that the increase was more marked for the early components and SI responses, while the changes in the late components and SII responses were more heterogeneous, especially at intensities greater than one times the MT. These results support the commonly accepted link between early SEP components and SI on one hand and the one between late components and SII on the other hand. However, none of these studies has combined EEG and MEG or has investigated the influence of the intensity of peripheral nerve stimulation on source activities in all brain cortex. Lastly, the intensity of peripheral nerve stimulation was not normalised or normalised using different methodologies (relative to MT or to the perceptual threshold [PT] or mixing both), while according to experimental setup and conditions, raw intensity (in mA) is not comparable from one subject to another and from one study to another. Furthermore, it has been shown that normalising the stimulus intensity to PT gave more consistent results regarding the size of SEPs (Fukuda et al., 2007) but this procedure has not been standardized across studies yet.

Consequently, the present study was designed to further investigate the origin and the characteristics of the late components, P60/N60 and P100/N100, in healthy conditions. Indeed, detailed examination of the late components would be an added value for the evaluation of the somatosensory integrations at higher processing level, involving extra sensorimotor cortical areas involved in cognitive processes (e.g., motor learning) and executive functions (e.g., motor planning). To this end, SEPs were produced by median nerve electrical stimulations delivered at the wrist level in neurologically intact participants. The stimulus intensity was normalised to PT and varied between 1.5 and 9 times the PT, that is, below and above MT (being between three and six times the PT according to our experience). EEG and MEG responses were recorded simultaneously and the time series were analysed within the time windows covering the first component P20/N20 and the late ones, P60/N60 and P100/N100. Source imaging for the three components was performed to identify the brain regions significantly activated by median nerve stimuli. Based on the localisation of MEG sources at the group level (given its greater

spatial accuracy compared with EEG; Baillet, 2017; Komssi et al., 2004; Leahy et al., 1998), we determined the regions of interest (ROIs) to compare the source activities according to the stimulus intensity. Statistical analyses were undertaken to compare the characteristics (source location and relationship with stimulus intensity) of early and late responses, their possible links and the interaction between cortical areas (ROIs) involved in these responses.

## 2 | MATERIALS AND METHODS

### 2.1 | Ethical statement

The study was conducted in accordance with the latest revision of the Declaration of Helsinki. The procedures were approved by the CNRS ethic committee (study #1402) and by the national ethical authorities (CPP Ile de France, Paris 6 – Pitié-Salpêtrière and ANSM; IRB 2015-A00462-47). All subjects provided their written informed consent prior to their inclusion in the research protocol. The data that support the findings of this study are available on request from N. G. among the authors; they are not publicly available due to ethical restrictions.

### 2.2 | Participants

The inclusion criteria were as follows: (i) no drug intake affecting the neural excitability (psychotropic drugs), (ii) no history of stroke, head trauma, heart disease, peripheral neuropathy or diabetes, and (iii) no metal implant or pacemaker. Twenty-two healthy subjects were included in the protocol. EEG and MEG recordings could not be performed in one of them due to ferromagnetic incompatibility (dental implants), and in two others, the anatomical magnetic resonance imaging (MRI) could not be segmented properly because of motion artefact. Accordingly, the data set in the present study included 19 subjects: 13 females and 18 right-handed participants (Oldfield, 1971), with age ranging between 22 and 61 years old (mean  $\pm$  standard error:  $32.5 \pm 2.6$  years old). The experiments were performed at the Centre of Neuroimaging Research (CENIR)-EEG/MEG Centre of the Brain Institute (ICM, Pitié-Salpêtrière Hospital, Paris, France).

### 2.3 | Simultaneous EEG/MEG

Elekta<sup>®</sup> Neuromag (TRIUX, Stockholm, Sweden) allowing synchronous EEG and MEG recordings was used.

EEG cap with 74 Ag/AgCl annular electrodes was placed according to the international 10/20 system (EasyCap GmbH, Herrsching, Germany; Nuwer 2018). It was positioned so that the Cz electrode was over the anatomical vertex point in each volunteer. Water-soluble conducting gel was injected in each electrode, and impedance was checked individually ( $\sim 5\text{--}10\text{ k}\Omega$ ) before acquisition. Single-use pregelled Ag/AgCl electrodes (Ambu<sup>®</sup> Neuroline 720, Ballerup, Denmark) were placed over the right ear lobe for the reference electrode and on the left scapula for the ground electrode. MEG included 306 superconducting quantum interference devices with 102 radial magnetometers and 204 axial gradiometers on the scalp.

Anatomical landmarks were captured including nasion, left and right preauricular points and up to 70 points over the scalp with a three-dimensional scanning system (Polhemus 3D Fastrak, Colchester, VT, USA) to digitalise the head shape of each volunteer. EEG electrode location was also recorded. Two head position indicator (HPI) coils were placed on the superior part of the forehead, on the right and the left sides and, two other ones, on the right and left mastoids. Before each recording session, a weak alternating current was injected in the HPI coils (electrically isolated from the subject), to generate a magnetic field captured by MEG sensors. This field was used to detect the position of HPI coils in the MEG helmet and to ensure that head position did not change between each acquisition. All the procedure (head shape digitalisation, location of EEG electrodes and HPI coils) allowed to reconstruct the head position in the MEG–EEG devices.

The electrooculogram (EOG) and the electrocardiogram (ECG) were recorded simultaneously, to get a continuous recording of noncerebral electrophysiological activities. These recordings were performed using single-use pregelled electrodes (same type of electrodes as the reference and ground electrodes) placed above and below the right eye and on the right and left temples for EOG and on the right clavicle and the left part of lower abdomen for ECG.

The amplifiers and the entire electronic part of the EEG system (also collecting EOG and ECG) were integrated into the MEG system, using the same internal clock to synchronise all acquisitions. Therefore, all signals (EEG, MEG, EOG and ECG) were collected simultaneously. All signals were filtered (1000 Hz lowpass filter for all, .03 Hz high-pass for EEG and .1 Hz high-pass for EOG and ECG) and digitalised using 3 kHz sampling rate.

## 2.4 | Experimental procedure

After the subjects were prepared for EEG, EOG and ECG recordings outside the shielded MEG room, they were

comfortably installed in the MEG chair whose position was adjusted so as the top of their head touched the top of the MEG helmet. All the electrodes for EEG, EOG, ECG and the HPI coils were connected to the EEG–MEG system. Stimulating electrodes (two .5 cm<sup>2</sup> silver plates; 1 cm apart) were placed over the median nerve, on the right side, at the wrist level (cathode proximal to the spinal cord), and they were connected with shielded cables to the electrical stimulator (DS7A, Digitimer Ltd, Hertfordshire, UK) located outside the MEG room. Percutaneous electrical stimuli (1 ms duration) were first delivered in order to evaluate PT. The intensity was increased progressively until the subject felt paraesthesia in the hand (cutaneous field of median nerve). The intensity was then decreased and increased three to five times successively, in order to determine precisely the minimal intensity for paraesthesia and local sensation below the stimulating electrodes. During recordings, the stimulation intensity was set at 1.5, 3, 6, and 9 times the PT; the maximum intensity (nine times the PT) was described by all subjects as unpleasant but not painful. The participants were instructed to stay as relaxed as possible during recordings, not moving, no swallowing and not clenching the jaw. Cameras and microphones were installed in the MEG room to maintain the contact with the subjects; videos and discussions were not recorded.

The protocol included eight recording sessions during which the subjects were asked to fix a cross on the wall in front of them and to limit eye blinks. They were also instructed not to count the stimuli, which interferes with SEP size (Mauguière et al., 1997). Each recording session started with a 5 s resting state acquisition (without stimulation) before triggering stimuli using a sequencer developed in Matlab<sup>®</sup> (The MathWorks, Inc., Natick, MA, USA), which delivered time-locked triggers to the electrical stimulators and synchronised event markers to the EEG–MEG acquisition system. Each session consisted of 300 median nerve stimulations delivered with interstimulus interval (ISI) randomly set between 500 and 600 ms (on average 555.8 ms). This ISI exceeds the time needed for EEG and MEG signals to return to baseline after stimulation; no significant changes were observed after 200 ms, that is, within the time for somatosensory integration (Mauguière, 2005; Mauguière et al., 1997; Figure 1a,b). Moreover, it has been reported that stimulus rates of up to 8 Hz can be used without significant loss in detectability of most components (Pratt et al., 1980) and that P20/N20 is not sensitive to ISI duration (Forss et al., 1995; Mauguière et al., 1997). Much less is known about late components, and P100/N100 in particular, but it was necessary to keep the same procedure for valid correlation analysis between the different components and the cortical areas activated; the stimulation frequency

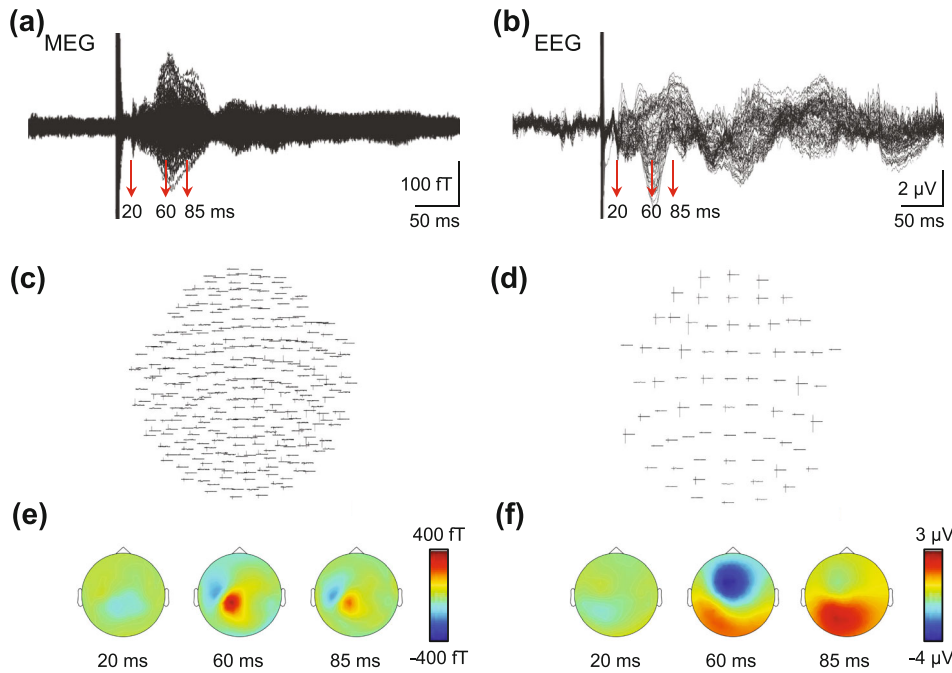


**FIGURE 1** Raw magnetoencephalogram (MEG) and electroencephalogram (EEG) epochs in one individual. Superimposition of the mean epochs ( $n = 600$  stimuli) at the level of each MEG (a) and EEG (b) sensor, around median nerve stimulation adjusted at six times the perceptual threshold. Mean epochs at the level of each sensor over the brain cortex in MEG (c) and EEG (d). Topography of the mean MEG (e) and EEG (f) activities, according to the corresponding gradient of colours, 20 ms (left figurine), 60 ms (middle figurine) and 85 ms (right figurine) after median stimulation (indicated in a and b by vertical red arrows).

between 1.6 and 2 Hz was a good compromise between optimal ISI duration and total duration of recordings (for subject comfort). Stimulation intensity was kept constant during one recording session and randomly changed from one session to another. Four intensities were tested (1.5, 3, 6, and 9 times the PT), and two recording sessions were performed at each intensity. Thus, eight recording sessions (2 runs  $\times$  4 stimulation intensities) were performed, and we collected a total of 600 conditioned signals at each of the four intensities tested. Including installation time, the total duration of the EEG/MEG experiment was about 2 h, plus 15 min for MRI.

## 2.5 | Anatomical MRI

MRI was performed to obtain anatomical brain images for each participant (Magnetom TRIO 3T, Siemens Munich, Germany; CENIR, Brain Institute, Pitié-Salpêtrière Hospital, Paris, France). The MRI images were obtained following a protocol adapted for MEG experiments: T1 weighting MPAGE sagittal orientation, flip angle =  $9^\circ$ , TE = 2.22 ms, TR = 2400 ms, TI = 1000 ms, voxel size =  $.8 \times .8 \times .8$  mm, matrix =  $320 \times 300$  and 256 contiguous slices. To avoid subject magnetisation, MRI acquisition was performed after EEG–MEG acquisitions. Images were segmented using FreeSurfer (<https://surfer.nmr.mgh.harvard.edu>) to reconstruct brain images that were used to localise the source activity in each individual. During segmentation, FreeSurfer registered the individual cortical surfaces in three atlases (Desikan–Killiany, Destrieux and Brodmann). These atlases are implemented in

Brainstorm software used for the source analysis (Tadel et al., 2011, 2019). The anatomical landmarks (nasion, left and right preauricular points, the anterior and posterior commissures and an interhemispheric point) were manually defined on the MRI images.

## 2.6 | Time series analysis

### 2.6.1 | Preprocessing

MEG time series were first filtered from external noises using MaxFilter (Elekta Neuromag, Helsinki, Sweden). The EOG was then used to detect eyes blink artefacts in both EEG and MEG signals. Independent component analysis (Fieldtrip toolbox, Matlab<sup>®</sup>) was performed to remove the EEG/MEG components that had the largest significant correlation coefficient with EOG. Then, ECG was used to detect and remove heart artefacts in MEG signals using principal component analysis (dataHandler, a software developed by the EEG/MEG centre of CENIR, Brain Institute, Pitié-Salpêtrière Hospital, Paris, France).

### 2.6.2 | Epoching and averaging

We visually checked for the appropriate removal of ocular and cardiac signals (EOG and ECG), the absence of edge effects that could occur during signal correction and the absence of electromyographic activity from other sources (facial and/or cranial muscles) interfering with EEG/MEG signals. Then, EEG and MEG were epoched

using a 500 ms window time-locked to stimulus: 100 ms before ( $-100$  ms) and 400 ms after the stimulus. EEG and MEG epochs from each acquisition were averaged (averaging of 300 epochs per run of acquisition), and the mean epochs from the two runs obtained at the same intensity were then averaged. Figure 1a,b shows the superimposition of the mean epochs obtained at the level of each MEG (Figure 1a) and EEG sensors (Figure 1b) in one participant.

### 2.6.3 | Source analysis

The realistic head model based on the symmetric boundary element method was used for the forward problem using OpenMEEG in Brainstorm (Matlab<sup>®</sup>; Gramfort et al., 2010; Kybic et al., 2005) which enables reliable source location, especially for EEG (Antonakakis et al., 2019; Lanfer et al., 2012). The boundary element method model was computed using the MRI of each individual to include the surfaces representing the boundaries between the tissues used in the model: scalp (head–air interface), outer skull (scalp–skull interface) and inner skull interfaces (interface between skull and brain, including cerebrospinal fluid). According to the guidelines in Brainstorm, we selected all the layers for EEG and only the inner skull layer for MEG (giving rise to similar results as using all layer), and we used adaptive integration (more accurate solution). For each subject and intensity, a noise covariance matrix was calculated on the prestimulus time window ranging from  $-100$  to  $-30$  ms (excluding the stimulus artefact) using the 600 epochs in the two runs of acquisition corresponding to that subject and intensity. Mean MEG and EEG epochs (in each individual and at each intensity tested) were then used to analyse the sources using weighted minimum norm estimation with unconstrained source orientation (Baillet, 2017; Baillet et al., 1999; Hämäläinen & Ilmoniemi, 1994; Tadel et al., 2011, 2019). We obtained the time courses of three orthogonal dipoles. The norm of their vectorial sum was then computed, yielding time courses of cortical current density. Finally, we calculated the corresponding  $Z$ -scores with respect to prestimulus baseline (noise covariance matrix).

### 2.6.4 | Windows of analysis corresponding to early and late components

The time windows covering the early (P20/N20) and late source components (P60/N60 and P100/N100) were determined according to our previous results (Sangari et al., 2016) and the grand average (19 participants) of the time course of normalized ( $Z$ -scored) current densities in

EEG and MEG. According to previous studies (Allison et al., 1991; Mauguiere, 2005; Passmore et al., 2014), we selected the results over the left SI (contralateral to stimulation site; Figure 2a,b), obtained at six times the PT (selected according to our preliminary analyses showing this intensity was optimal; see Section 3). The resulting time windows to calculate the mean current density for each component were as follows: 17 to 21.5 ms after stimulus trigger for P20/N20, 48 to 71 ms for P60/N60 and from 72 to 99 ms for P100/N100. The  $Z$ -scores of the mean current density during these time windows were extracted in each individual for group analysis.

### 2.6.5 | Identification of ROIs

$Z$ -scores of current densities calculated in each individual between  $-100$  and 400 ms around stimuli were spatially projected into the standard Montreal Neurological Institute template to visualise the mean location of mean source activities in the group (grand average). ROIs were defined in light of MEG activity at six times the PT during the time windows covering P20/N20, P60/N60 and P100/N100 and were delineated according to the Desikan-Killiany and Brodmann atlases implemented in Brainstorm (premotor and SII areas were manually defined according to Brodmann areas). The resulting atlas was used to compute  $Z$ -scores in corresponding cortical regions in each individual according to their own anatomies (the atlas was projected onto individual MRIs), during early and late SEPs.

## 2.7 | Statistical analysis

We identified a total of 21 ROIs over the left (contralateral to the stimulation site) and right (ipsilateral) hemispheres for the two modalities of recordings (same ROIs for EEG and MEG). We thus performed a Bonferroni correction to determine the minimum  $Z$ -score ( $\geq 4.02$ ) to consider for statistical significance (Figures 2c–h and 3).

Linear mixed models were built with subjects as random effect and modality (MEG and EEG), intensity (the four intensities tested), ROI (the 13 considered as significantly activated after Bonferroni correction) and component (P20/N20, P60/N60 and P100/N100) as fixed effects. Age and PT were also tested as covariables. We made sure that the underlying assumptions (normality, homoscedasticity and absence of outliers) were valid and  $p$ -values were calculated after false discovery rate correction. According to the results of the model, post hoc pairwise analyses were performed using Student's  $t$ -tests on least-squares means of normalized current densities ( $Z$ -scores).

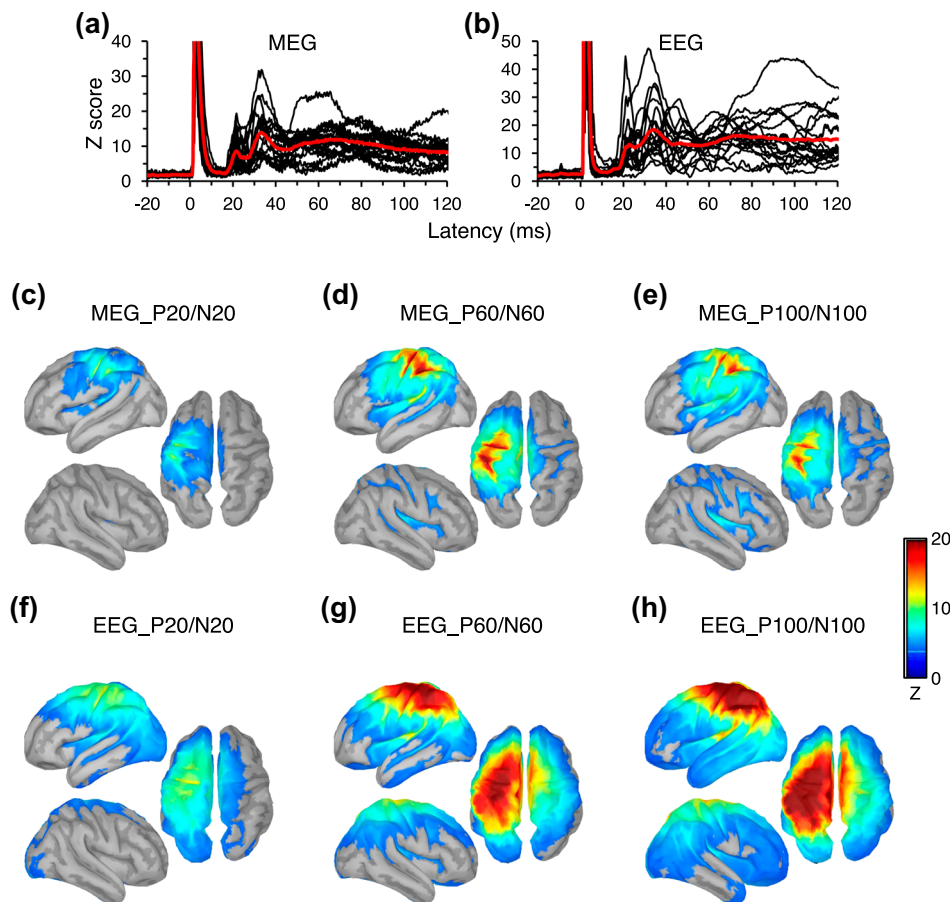


**FIGURE 2** Mean normalised magnetoencephalogram (MEG) and electroencephalogram (EEG) source activities in the brain cortex during early and late somatosensory evoked potentials. Time course of mean normalised current in each individual (black lines) and their grand average around median nerve stimulation adjusted at six times the perceptual threshold (red line; between  $-20$  and  $120$  ms): The Z-scores of current densities were extracted after MEG (a) and EEG (b) source analyses, at the level of the post-central cortex corresponding to the primary somatosensory area. Each black trace corresponds to the results of one participant, and the red line results from the grand average of the 19 participants. Normalised source activity from MEG (c and e) and EEG (f and h) in the group of participants ( $n = 19$ ) with, in each figurine, upper left, the left hemisphere, lower left, right hemisphere, and on the right, the top view of the brain. The Z-score of mean current density was extracted for each window of analysis corresponding to P20/N20 (c and f), P60/N60 (d and g) and P100/N100 (e and h) in each individual and projected into the common Montreal Neurological Institute space. The gradient of colours corresponds to Z-scores from 0 (dark blue) to 20 (dark red), with a threshold estimated at Z-score = 4.02 after  $p$ -value correction (Bonferroni correction for multiple comparisons; thin line within the blue area in the legend). Accordingly, only significant activity ( $p$ -value  $< 0.000058$ ) are illustrated ( $>20\%$  of the maximum amplitude of the gradient).

We also investigated the correlations between SEP components and between ROIs during each component. More specifically, we assessed the relationship between Z-scores corresponding to the same ROI but different SEP components using Spearman's rank correlation coefficient. A threshold of  $r = 0.7$  was chosen both to select high-intensity correlation and take into account multiple testing of correlations (conservative Bonferroni correction). Partial correlations were processed to determine ROIs which activity were closely linked between groups of regions. Lastly, we performed cluster analysis using classification methods based on local singular value decomposition.

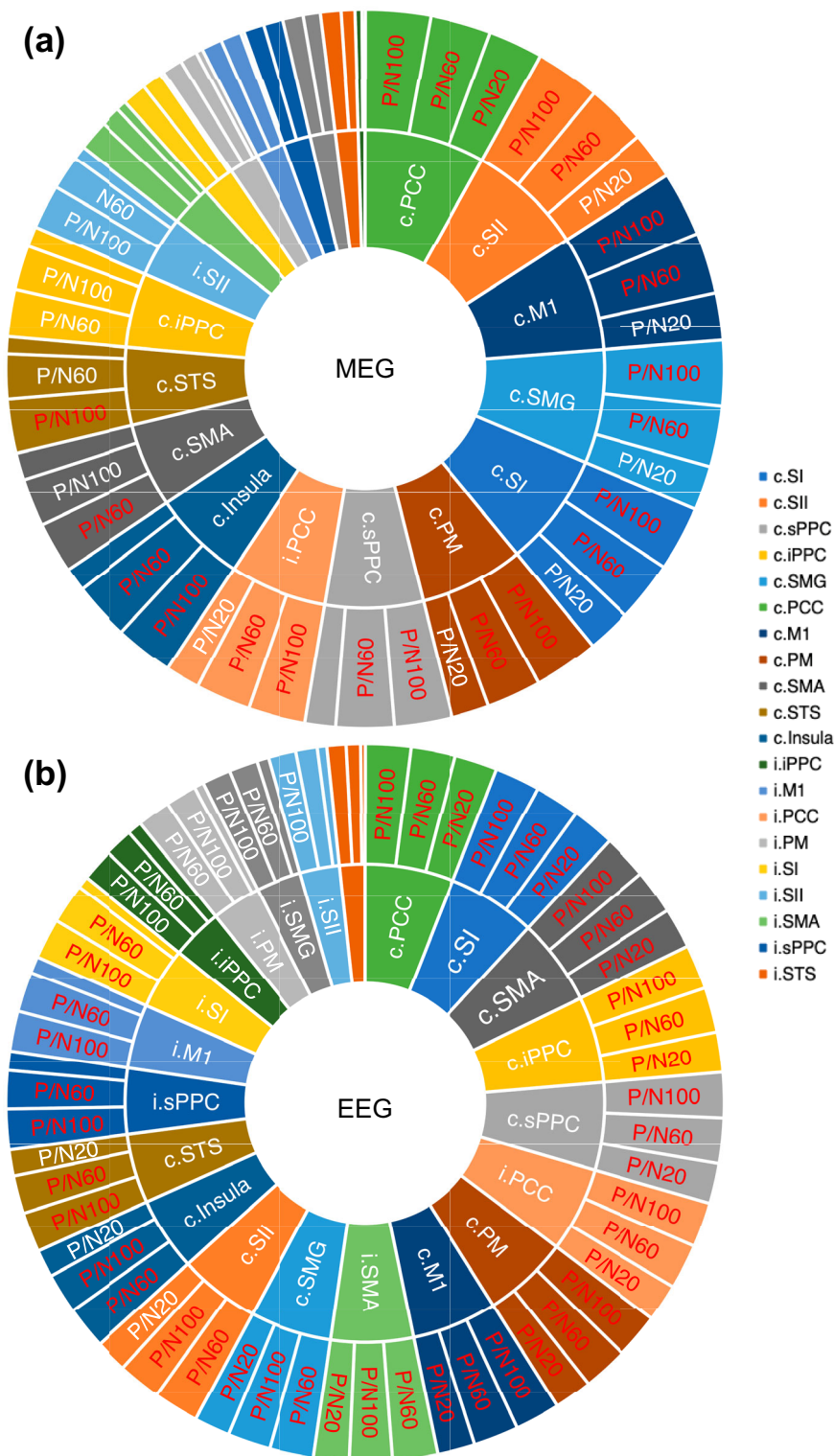
Statistical analyses were performed with JMP software<sup>®</sup> (SAS Inc., Cary, NC, USA). All tests were two-sided. A  $p$ -value  $\leq 0.05$  was considered statistically significant. Data were reported as mean  $\pm$  one standard error for continuous variable and as frequency (%) for categorical variables. For better readability, all tests and parameters are specified in Section 3.

### 3 | RESULTS

Figure 1 shows MEG and EEG raw data obtained at six times the PT from one representative participant, with the



**FIGURE 3** Hierarchy of activated brain areas in the group. The regions of interest are organised according to the proportion of subjects in the group ( $n = 19$ ) with magnetoencephalogram (MEG) (a) and electroencephalogram (EEG) (b) activities after median nerve stimulation (six times the perceptual threshold) significantly different from baseline ( $Z$ -score  $\geq 4.02$ ,  $p$ -value  $< 0.000058$ ). Each level of the hierarchy is represented by one ring and the larger the part of the ring per item, the greater the proportion of subjects with significant  $Z$ -score. The first level of hierarchy includes the regions of interest in the contralateral (c.) and ipsilateral (i.) hemispheres. The second level includes the three components. The proportions  $\geq 50\%$  are indicated in white and those  $\geq 75\%$  in red. iPPC, inferior posterior parietal cortex; M1, primary motor cortex; PCC, posterior cingulate cortex; PM, premotor cortex; SI, primary somatosensory area; SII, secondary somatosensory area; SMA, supplemental motor area; SMG, supramarginal area; sPPC, superior posterior parietal cortex; STS, superior temporal sulcus.



superimposition of the mean epochs (Figure 1a,b) and their mean at the level of each sensor over the scalp (Figure 1c,d). Figure 1e,f shows the topography of the signal at 20, 60 and 85 ms, that is, within the analysis windows corresponding to P20/N20, P60/N60 and P100/N100, respectively. For both MEG and EEG topographies, most

activity manifested in the left side, contralateral to stimulation site, and during P60/N60. Specifically, parietal regions were primarily activated at 20 ms (P20/N20) and fronto-parietal ones at later latencies. Source analysis and  $Z$ -score normalisation of mean current density were performed in each individual for the following group analyses.

### 3.1 | Source imaging

Source analysis resulted in the estimation of mean current density each at .33 ms, between  $-100$  and  $400$  ms around stimulation, which was then transformed into  $Z$ -score for group analysis. Figure 2a,b shows MEG (a) and EEG (b)  $Z$ -scores over the left SI area (post-central gyrus), around median nerve stimuli adjusted at six times the PT; each black trace shows the  $Z$ -scores in each participant ( $n = 19$ ) and the red trace the mean  $Z$ -scores in the group. On average, peaks of activity occurred at about  $22$  and  $35$  ms after peripheral stimuli, corresponding to early SEPs  $<40$  ms, and activity slowly increased again at about  $45$  ms in MEG and  $55$  ms in EEG, until  $100$  ms in MEG and longer in EEG, corresponding to late SEPs  $>40$  ms.

$Z$ -scores of the mean current density during the time windows covering P20/N20, P60/N60 and P100/N100 were extracted for each individual. Figure 2c–h shows the projection of MEG (c–e) and EEG (f–h)  $Z$ -scores in the common Montreal Neurological Institute space (only used for this grand average) in the three windows of analysis, P20/N20 (c and f), P60/N60 (d and g) and P100/N100 (e and h). According to Bonferroni correction for multiple comparisons, significant activity during P20/N20 was mostly observed over the left fronto-parietal cortex in both MEG and EEG maps (Figure 2c,f). At longer latency, during P60/N60 (d and g) and P100/N100 (e and h), the mean activity over the left sensorimotor cortex was greater as compared with P20/N20 and spread over prefrontal, inter-hemispheric and posterior parietal areas in the left (contralateral) and right (ipsilateral to stimulation site) hemispheres; the spreading being greater in EEG compared with MEG. The ROIs were then determined according to MEG activity (given its greater spatial accuracy compared with EEG; Baillet, 2017; Komssi et al., 2004; Leahy et al., 1998) during P60/N60 (greater activity as compared with P100/N100; cf. Figure 2d and e). Significant activity in the left hemisphere (contralateral to stimuli) was thus found in SI, SII (parietal operculum in the ceiling of the lateral sulcus, overlapping ventral part of areas 40 and 43), superior posterior parietal cortex (sPPC), inferior posterior parietal cortex (iPPC), supramarginal area (SMG), posterior cingulate cortex (PCC), superior temporal sulcus (STS), insula and over motor and premotor areas including the primary motor cortex (M1), the premotor cortex (PM) and the supplemental motor area (SMA). In the right hemisphere (ipsilateral to stimuli), significant activity was found in SI, SII, sPPC, iPPC, PCC, STS, M1, PM and SMA.

During P20/N20, the most significant MEG activity in Figure 2c was limited to the left (contralateral) hemisphere with (i) the central sulcus including in its posterior part, Brodmann's area 3a and b (part of SI) and, in

its anterior part, Brodmann's area 4 (M1), (ii) the sulcus at the intersection between SI, sPPC and SMG, and (iii) the upper part of the premotor areas. Similar results were observed in EEG but the activity was broader over the same areas (SI, M1, sPPC and SMA; Figure 2f). During P60/N60, the mean MEG activity increased in the same areas (contralateral SI, M1, sPPC and SMA) and was much clearer in SII, as well as in the other areas listed supra but to a lesser extent in these areas as compared with SI, M1, sPPC, SMA and SII (Figure 2d). The mean EEG activity was much greater than MEG and, again, much broader in the left contralateral hemisphere; the difference with MEG was even greater in the right—ipsilateral—hemisphere (Figure 2g). At longer latencies, corresponding to P100/N100, we observed similar results as during P60/N60, but the mean MEG activity was globally lower (Figure 2e) while the mean EEG activity increased again and was even broader.

Mean normalised epochs in Figure 2a,b indicate that there was a great interindividual variability (Ahn et al., 2015; Buchner et al., 1995). For EEG data, 28.6% of the total variance could be explained by between-SEP component variability, 20.3% by between-ROIs variability, 21.6% by between-subject variability and the 29.6% left by interactions which led to an interclass coefficient of 0.15. For MEG data, 31.0% of the total variance could be explained by between-SEP component variability, 10.7% by between-ROIs variability, 26.2% by between-subject variability and the 32.0% left by interactions which led to an interclass coefficient of 0.16. Therefore, we further investigated which regions were mainly activated in the group, by calculating the proportion of subjects with significant source activity in the different ROIs (still according to the  $Z$ -score threshold after Bonferroni correction). The sunburst charts in Figure 3 show the hierarchical distribution of MEG (Figure 3a) and EEG data in the group (Figure 3b). The first level of hierarchy corresponds to the brain regions and the second level to the SEP components: The larger the segment at a given level of the hierarchy, the greater the proportion of subjects with significant  $Z$ -score ( $>75\%$  of the participants with significant  $Z$ -scores in red and between 50% and 74% in white). The first result that came out from this analysis is that significant source activity was more consistent across subjects in the contralateral hemisphere in both MEG and EEG, as compared with ipsilateral hemisphere. Moreover, the reproducibility of the results across subjects was greater in EEG as compared with MEG. In addition, Figure 3b shows that EEG activity in the ipsilateral hemisphere was quite consistent across subjects at the latency of late components.

Table 1 summarises the data illustrated in Figure 3 to better highlight the common results in MEG and EEG

TABLE 1 Reliability of significant source activity.

		Areas	P20/N20		P60/N60		P100/N100	
			MEG	EEG	MEG	EEG	MEG	EEG
Hemisphere	Contralateral	SI	Dark	Dark	Dark	Dark	Dark	Dark
		SII	Dark	Dark	Dark	Dark	Dark	Dark
		M1	Dark	Dark	Dark	Dark	Dark	Dark
		SMA	Dark	Dark	Dark	Dark	Light	Light
		PM	Dark	Dark	Dark	Dark	Dark	Dark
		sPPC	Dark	Dark	Dark	Dark	Dark	Dark
	Ipsilateral	SI	Dark	Dark	Dark	Dark	Dark	Dark
		SII	Dark	Dark	Dark	Dark	Dark	Dark
		M1	Dark	Dark	Dark	Dark	Dark	Dark
		SMA	Dark	Dark	Dark	Dark	Dark	Dark
		PM	Dark	Dark	Dark	Dark	Dark	Dark
		sPPC	Dark	Dark	Dark	Dark	Dark	Dark
	iPPC	Dark	Dark	Dark	Dark	Dark	Dark	
	SMG	Dark	Dark	Dark	Dark	Dark	Dark	
	PCC	Dark	Dark	Dark	Dark	Dark	Dark	
	STS	Dark	Dark	Dark	Dark	Dark	Dark	

Note: Proportion of subjects with significant source activity (according to Z-score threshold after Bonferroni correction for multiple comparison) during P20/N20, P60/N60 and P100/N100 in MEG and EEG at the level of the regions of interest on both contralateral and ipsilateral hemispheres. Dark grey when more than 75% of the participants exhibited significant Z-score, light grey, between 50% and 75% and white when less than 50%.

Abbreviations: EEG, electroencephalogram; iPPC, inferior posterior parietal cortex; M1, primary motor cortex; MEG, magnetoencephalogram; PCC, posterior cingulate cortex; PM, premotor cortex; SI, primary somatosensory area; SII, secondary somatosensory area; SMA, supplemental motor area; SMG, supramarginal area; sPPC, superior posterior parietal cortex; STS, superior temporal sulcus.

source imaging. During P20/N20, significant activity was found in both modalities in the contralateral SI, SII, M1, PM and SMG and in PCC on both hemispheres. At longer latencies, during late SEPs, the results of source imaging were consistent between the two modalities in the contralateral hemisphere, while in the ipsilateral hemisphere, common activity was mostly found only in SII and PCC. In fact, ipsilateral EEG activity was almost entirely limited to the upper part of the hemisphere (Figure 2g,h), with no real demarcation between functional regions. In the lateral part, significant ipsilateral MEG activity could be observed at the group level in the central sulcus (SI–M1), PM, sPPC and STS (Figure 2e), but according to Figure 3a and Table 1, these results were not replicable in the major part of the participants.

The results of source imaging thus indicate that stimulus-induced activity during P20/N20 mostly occurred in contralateral SI, SII, M1, PM and SMG and in

PCC on both hemispheres. These regions were still activated at longer latencies, during late SEPs, P60/N60 and P100/N100, which are characterised, compared with P20/N20, by activity in contralateral SMA, sPPC, iPPC, STS and insula and ipsilateral SII. Video of source imaging (Video S1) reveals that the mean MEG activity in the group started 18 ms after stimuli, at the level of the central (SI–M1), pre-central (premotor areas) and post-central sulci (junction between SI, sPPC and SMG). Then, activity in SII and both contralateral and ipsilateral PCC occurred at 19–20 ms. At 22–23 ms, the activity decreased until 28 ms when it reincreased again in the same areas as during P20/N20 with greater and more obvious activity in contralateral PM, SII, sPPC, iPPC, STS and insula. Interestingly, ipsilateral MEG activity (right hemisphere) in SII started at about 28 ms, being particularly clear at 30 ms, decreasing at about 38 ms and reincreasing again about 56 ms, for being particularly significant between

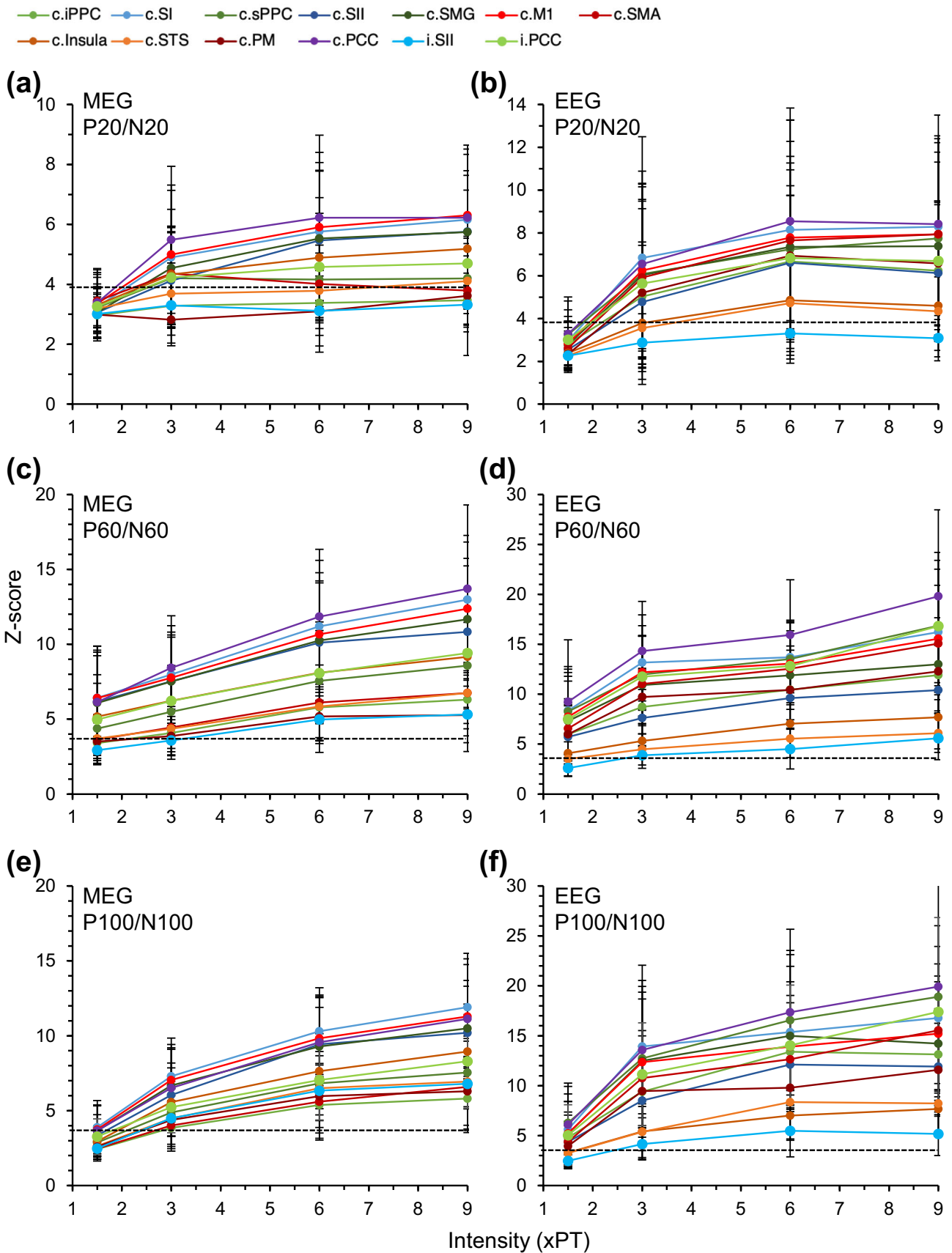


FIGURE 4 Legend on next page.

62 and 97 ms. Regarding EEG, activity mostly started at about 19 ms in contralateral central and pre-central sulci, reaching sPPC at 20 ms, and then increased and spread in other contralateral areas until 38 ms, when it decreased. It mostly reincreased again at about 60 ms for decreasing a bit at about 97 ms. In the ipsilateral hemisphere, EEG activity was much broader than MEG. If we focus our attention on ipsilateral SII, EEG activity started at 29 ms and was more significant at 59 ms until the end of the video. To sum up, the video indicates that the central sulcus is the first area to be activated during P20/N20 but activity in SII, PM, SMG and PCC on both sides quickly occurred within the duration of the time window for P20/N20. Then, activity in sPPC, iPPC, STS, insula and ipsilateral SII starts at about 30 ms and was still observed during late SEPs, P60/N60 and P100/N100. Therefore, and even if the activity decreased between early and late SEPs, all the cortical areas engaged in SEPs were activated at 30 ms.

In order to further investigate the characteristics of late components and the respective role of cortical areas in these responses, compared with P20/N20, we investigated the influence of stimulus intensity on the responses over these ROIs (contralateral SI, SII, M1, PM, SMA, SMG, sPPC, iPPC, STS, PCC, insula and ipsilateral PCC and SII).

### 3.2 | Influence of stimulus intensity

On average, PT was  $58.6 \pm 3.7 \mu\text{A}$ , ranging from 37 to  $95 \mu\text{A}$  (median value =  $58 \mu\text{A}$ ). Even if particular care was taken to estimate precisely PT in each individual, the measure depended on their concentration and their investment. Moreover, it has been reported that SEP amplitude increases with age (Desmedt & Cheron, 1980, 1981; Hagiwara et al., 2014; Huttunen, 1995; Kakigi & Shibasaki, 1991). We did not find any significant influence of PT on stimulation-induced cortical activities (linear mixed model,  $p$ -value = 0.08). The influence of age did not reach the level of statistical significance ( $p$ -value = 0.06) likely due to the fact that most of the participants were under 30 (14/19 participants). Lastly, a

gender effect has also been reported in previous studies, especially in EEG due to distinct volume conductor between males and females (MEG being not influenced by this parameter; Huttunen et al., 1999). However, given the number of subjects (13 females vs. 6 males) and the number of parameters in the model, the comparison was not valid. However, we observed higher values in females than in males, especially in EEG data (not in MEG). Even if the size of our study group did not allow to further investigate these parameters (age and gender effect), it is interesting that we were able to find similar characteristics as those reported in previous studies, on larger study groups.

Figure 4 illustrates the Z-scores of mean MEG (a, c and e) and EEG (b, d, and f) current density in the group, according to the intensity of the median nerve stimuli (times the PT), in contralateral (c.) SI, SII, M1, PM, SMA, SMG, sPPC, iPPC, STS, PCC, insula and ipsilateral (i.) PCC and SII, during the time window corresponding to the three components P20/N20 (a and b), P60/N60 (c and d) and P100/N100 (e and f). In all conditions, Z-score systematically increased between 1.5 and 3 times the PT (except in c.PM at the latency of P20/N20 in MEG). Further increase in stimulus intensity mostly led to further increase in Z-score except at the level of SMA (in MEG P20/N20; Figure 4a) or decrease at six times the PT and reincrease at nine times the PT (e.g., in SI, M1, SMA and sPPC using EEG; Figure 3a) or still increase at six times the PT and decrease at nine times the PT (e.g., in SII using EEG at the latency for P20/N20 and P60/N60; Figure 3a,c).

Repeated-measures linear mixed-effects model was computed to evaluate the influence of the intensity (1.5, 3, 6 and 9 times the PT) on the Z-score of mean current density taking into account the recording modality (MEG and EEG), the ROIs (contralateral SI, SII, M1, PM, SMA, SMG, sPPC, iPPC, STS, PCC, insula and ipsilateral [i.] PCC and SII) and the component (P20/N20, P60/N60 and P100/N100). Adjusted  $R^2$  was 0.98, and all fixed effects and their interactions were significant: false discovery rate-corrected  $p$ -value < 0.001 for all regressors and interactions except for that between intensity, recording modality and component for which  $p$ -value < 0.05. Least-

**FIGURE 4** Relationship between stimulus intensity and normalised source activity in early and late somatosensory evoked potentials. The Z-scores of mean current density ( $n = 19$  participants) in magnetoencephalogram (MEG) (a, c, e) and electroencephalogram (EEG) (b, d, f), in the three windows of analysis corresponding to P20/N20 (a and b), P60/N60 (c and d) and P100/N100 (e and f) for the main areas activated are plotted against the intensity of the median nerve stimulation, normalised to the perceptual threshold (times perceptual threshold [PT]). Interrupted lines indicate the threshold for significant Z-score ( $\geq 4.02$ , according to Bonferroni correction for multiple comparisons). Vertical bars are  $\pm 1$  SD. iPPC, inferior posterior parietal cortex; M1, primary motor cortex; PCC, posterior cingulate cortex; PM, premotor cortex; SI, primary somatosensory area; SII, secondary somatosensory area; SMA, supplementary motor area; SMG, supramarginal area; sPPC, superior posterior parietal cortex; STS, superior temporal sulcus.

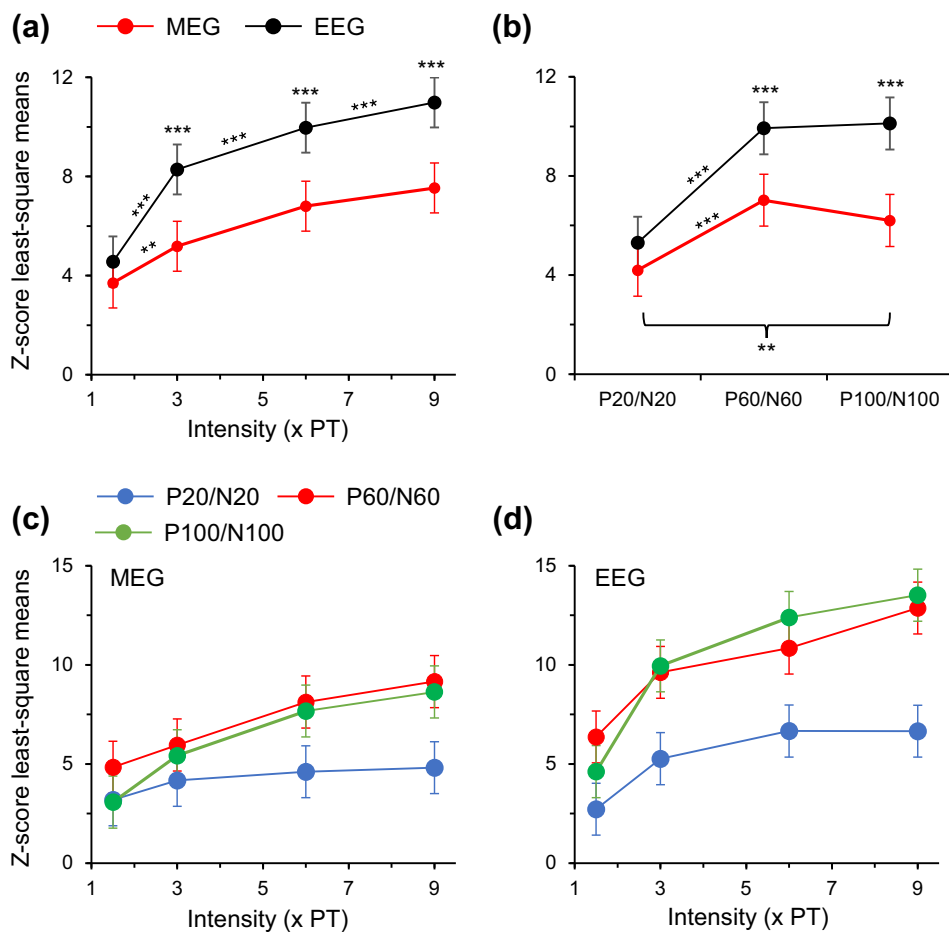


**FIGURE 5** Prediction of magnetoencephalogram (MEG) and electroencephalogram (EEG) early and late components according to the stimulus intensity. Z-score least-squares means from the repeated-measures linear mixed-effects model are plotted against the intensity of median nerve stimulation (normalised to the perceptual threshold [PT], times the PT; a, c, d) or the somatosensory evoked potential components (b) extracted from MEG (red dots and lines in a and b) and EEG source analysis (black dots and lines in a and b), at the latency of P20/N20 (blue dots and lines in c and d), P60/N60 (red dots and lines in c and d) and P100/N100 (green dots and lines in c and d) from MEG (c) and EEG (d). Vertical bars are  $\pm 1$  SD. \*\*\* $p$ -value  $< 0.001$ , \*\* $p$ -value  $< 0.01$  after post hoc comparisons of two means (Student's  $t$ -tests on least-square means; in a and b).  $P$ -values for c and d are indicated in Table 2.

**TABLE 2** Post hoc comparisons of components according to the intensity.

		1.5 × PT	3 × PT	6 × PT	9 × PT
MEG	P20/N20 versus P60/N60	0.025	0.0152	<0.0001	<0.0001
	P20/N20 versus P100/N100	0.8740	0.0871	<0.0001	<0.0001
	P60/N60 versus P100/N100	0.0167	0.4608	0.5298	0.4714
EEG	P20/N20 versus P60/N60	<0.0001	<0.0001	<0.0001	<0.0001
	P20/N20 versus P100/N100	0.099	<0.0001	<0.0001	<0.0001
	P60/N60 versus P100/N100	0.0171	0.6464	0.0353	0.3702

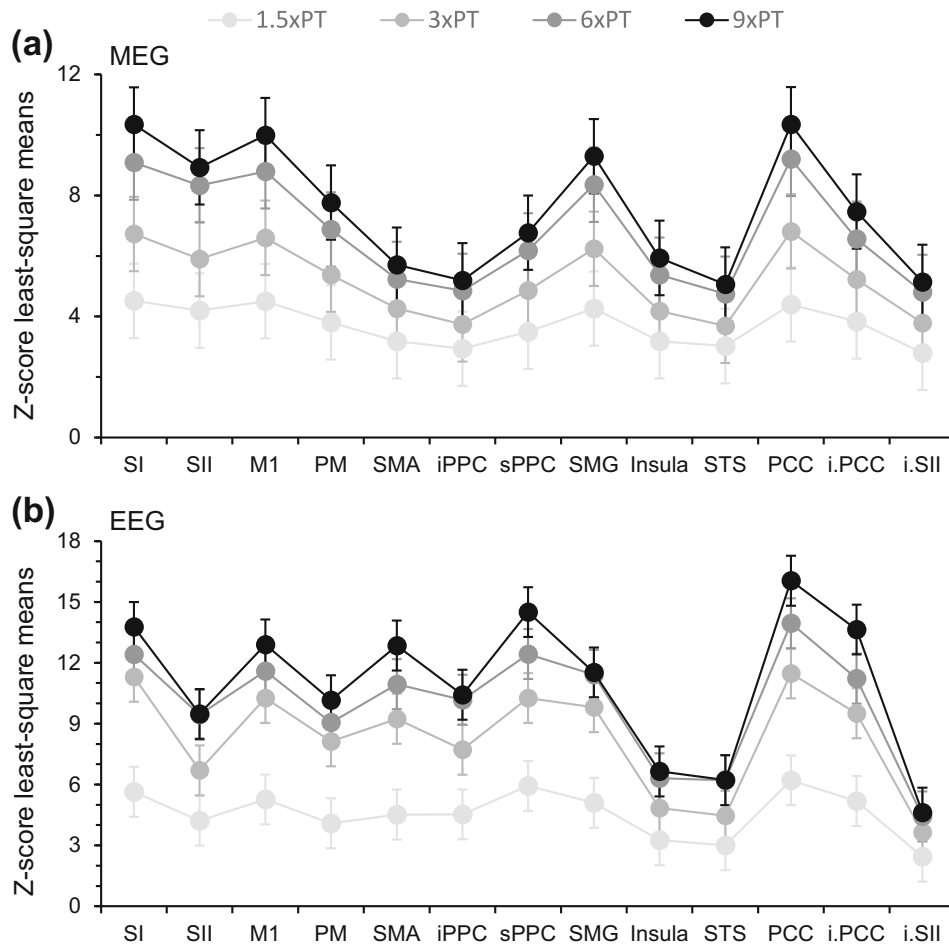
Note:  $p$ -values of post hoc Student's  $t$ -tests comparing Z-score least-squares means between components according to the intensity of median nerve stimulation. Squares in grey indicate nonsignificant differences.

Abbreviations: EEG, electroencephalogram; MEG, magnetoencephalogram; PT, perceptual threshold.

squares means of Z-scores were then used to illustrate the interactions between factors, which best represents the model prediction (taking into account all factors) and gives a much greater readability of the influence of the stimulus intensity on MEG and EEG activities and their location during early and late components. Post hoc pairwise comparisons of least-squares means were performed using Student's  $t$ -tests. Figure 5 shows that least-squares means were significantly greater for EEG than for MEG above three times the PT (Figure 5a;  $p$ -value  $< 0.001$ ) and

much more similar between late components (P60/N60 and P100/N100) compared with early one (P20/N20; Figure 5c,d); differences between P60/N60 and P100/N100 being mostly nonsignificant contrary to those between P20/N20 and the two late components (see  $p$ -values in Table 2). The similarity between late components is also shown in Figure 5b; differences between late component being nonsignificant ( $p$ -value = 0.17 in MEG and 0.74 in EEG). This figure also indicates that during P20/N20, there was no significant differences between

**FIGURE 6** Prediction of the influence of stimulus intensity in regions of interest. Z-score least-squares means from the repeated-measures linear mixed-effects model calculated at 1.5 (light grey dots and lines), 3 (middle grey dots and lines), 6 (dark grey dots and lines) and 9 times the perceptual threshold (PT) (black dots and lines) are plotted against the regions of interest for magnetoencephalogram (MEG) (a) and electroencephalogram (EEG) (b). Vertical bars are  $\pm 1$  SD. iPPC, inferior posterior parietal cortex; M1, primary motor cortex; PCC, posterior cingulate cortex; PM, premotor cortex; SI, primary somatosensory area; SII, secondary somatosensory area; SMA, supplemental motor area; SMG, supramarginal area; sPPC, superior posterior parietal cortex; STS, superior temporal sulcus.



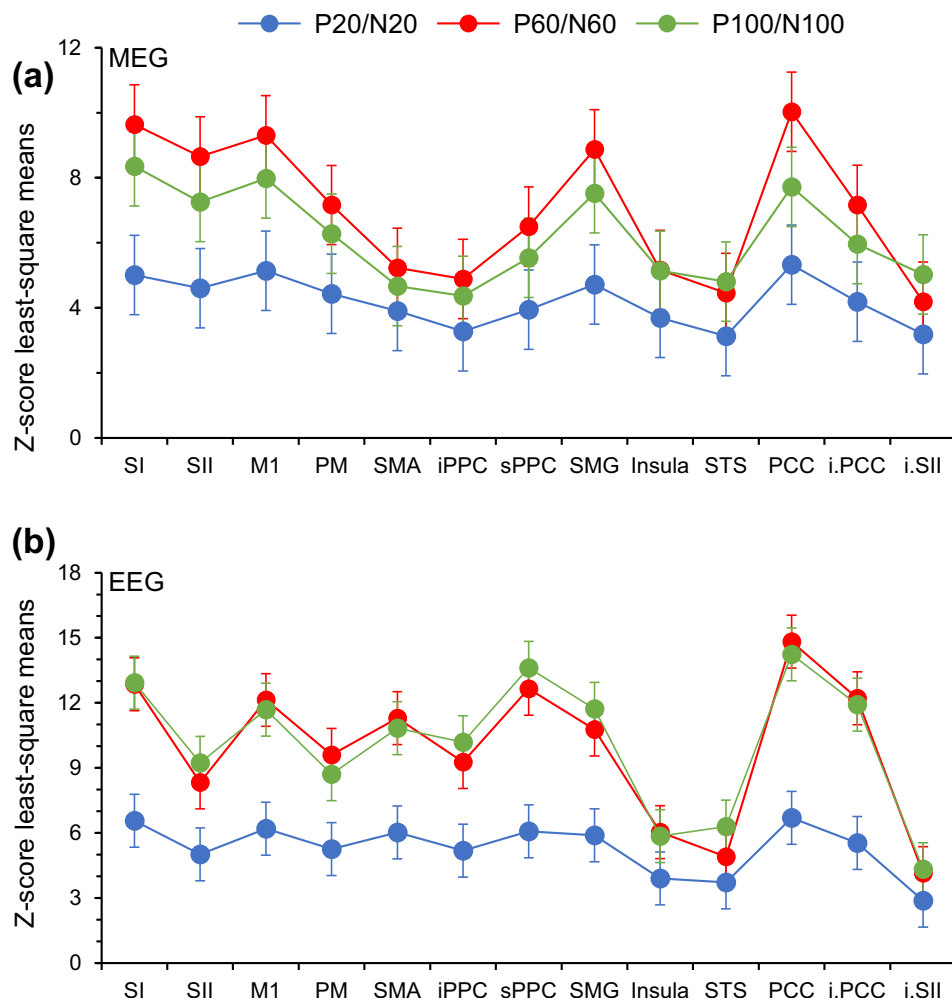
MEG and EEG ( $p$ -value = 0.1). The model thus indicates greater activity in EEG than in MEG at intensity greater than or equal to three times the PT but the difference between the two modalities mostly manifests during late components; MEG and EEG activities being comparable during P20/N20. Furthermore, the model reveals similar influence of stimulus intensity on late components but different from P20/N20.

Figure 6 illustrates the interaction between the recording modalities, the stimulus intensity and the ROIs. According to the model, MEG activity increased mostly similarly between 1.5 and 6 times the PT whatever the ROIs (Figure 6a), but there was a steep increase in EEG activity between 1.5 and 3 times the PT (Figure 6b). This result is also illustrated in Figure 5a showing that the slope between 1.5 and 3 times the PT is greater for EEG compared with MEG. Between six and nine times the PT, both MEG and EEG activities still increased but to a much lesser extent, especially in MEG, compared with the difference between three and six times the PT. This result suggests that SEPs plateaued at intensity greater than or equal to three times the PT in MEG and greater than or equal to six times the PT in EEG; see also Figure 5a and the nonsignificant differences in MEG,

between three and six ( $p$ -value = 0.06) and between six and nine times the PT ( $p$ -value = 0.15). After post hoc pairwise comparisons, the conditions with similar results were clustered, and we found similar grouping in MEG and EEG including the following: (i) at three times the PT, PPC-SI and SMG-M1, (ii) at six times the PT, SI-M1-SMG, and (iii) at nine times the PT, SI-M1.

Figure 7 illustrates the interaction between the recording modalities, the components and the ROIs. Results at the latency of late components are more similar than those at the latency of P20/N20, especially in EEG (Figure 7b; as illustrated in Figure 5c,d). Moreover, Figure 7 shows comparable results in some ROIs depending on the component and the recording modalities. We thus compared the clusters after post hoc pairwise comparisons to identify ROIs with comparable results in both MEG and EEG: (i) at the latency of P20/N20, SI-M1-SMG, and (ii) at the latency of P60/N60, SI-M1 and STS-i.SII; we did not find any common cluster at the latency for P100/N100.

Whether for stimulus intensity or component, similar results were observed between S1, M1 and SMG suggesting that activities within these areas were likely particularly linked. To further investigate the relationships between ROIs during early and late components, we



**FIGURE 7** Prediction of early and late components in regions of interest. Z-score least-squares means from the repeated-measures linear mixed-effects model calculated at the latency of P20/N20 (blue dots and lines), P60/N60 (red dots and lines) and P100/N100 (green dots and lines) for magnetoencephalogram (MEG) (a) and electroencephalogram (EEG) (b). Vertical bars are  $\pm 1$  SD. iPPC, inferior posterior parietal cortex; M1, primary motor cortex; PCC, posterior cingulate cortex; PM, premotor cortex; SI, primary somatosensory area; SII, secondary somatosensory area; SMA, supplemental motor area; SMG, supramarginal area; sPPC, superior posterior parietal cortex; STS, superior temporal sulcus.

performed correlation analysis at the optimal intensity six times the PT (for both MEG and EEG and in most ROIs).

### 3.3 | Correlation between SEP components and between ROIs

Correlation analyses were performed to evaluate the statistical links between ROIs and SEP components when stimulus intensity was set at six times the PT. Regarding the correlation between early and late components, we did not find any significant correlation in MEG activities between early and late components in ROIs significantly activated. In EEG, we found only significant correlation ( $r > 0.7$ ) between P20/N20 and P100/N100 at the level of (i) STS (P100/N100) and sPPC (P20/N20;  $p$ -value  $< 0.0001$ ), (ii) STS (P100/N100) and iPPC (P20/N20;  $p$ -value  $< 0.001$ ), (iii) PCC (P100/N100) and M1 (P20/N20;  $p$ -value  $< 0.001$ ), (iv) STS (P100/N100) and sPPC (P20/N20;  $p$ -value  $< 0.001$ ), (v) STS (P100/N100) and M1 (P20/N20;  $p$ -value  $< 0.001$ ) and (vi) STS (P100/N100) and SI (P20/N20;  $p$ -value  $< 0.001$ ).

We also studied the link between ROIs within each component using partial correlation which measured the degree of association between ROIs considering the other ones. For MEG-P20/N20, we found significant link between SI and M1 and M1 and PM. For MEG-P60/N60, we found significant correlations between M1, PM and SII; SMG was also linked to SI and to SII but activity in SI and SII were not significantly correlated. Lastly, for MEG-P100/N100, we found significant correlations between SI and M1, SI and SMG, M1 and PM, M1 and sPPC and PM and SMA.

For EEG-P20/N20, we still found significant correlation between SI and M1. We also found significant link between activities in SI and SMG, SII and SMG, sPPC and iPPC and STS and iPPC. For EEG-P60/N60, we found significant correlation between SI and SMG, SI and M1, M1 and PM, PM and SII and SII and SMG. Lastly, for EEG-P100/N100, we found again significant correlations between SI and SMG, SI and M1, M1 and PM and SII and insula.

This analysis confirms that the correlation between early and late components is sparse and, most importantly,



that there is very limited or even no link between early and late (only some between P20/N20 and P100/N100). Accordingly, the most reliable linked MEG/EEG activities between ROIs include SI-M1 and M1-PM at the latency of P20/N20 and P100/N100. P60/N60 is distinguished by other correlations including for the most reliable M1-PM-SII, SI-SMG and SII-SMG. At the latency of P20/N20, EEG activities in associative cortices were significantly linked (sPPC-iPPC and STS-iPPC).

### 3.4 | Clusters of cortical activity

Last part of the statistical analysis consisted of running classification methods based on a local singular value decomposition followed by a clustering algorithm which divided iteratively the clusters of variables (SEP components and ROIs, stimulus intensity at six times the PT) and reassigned the variables to clusters until it was not possible to split the clusters. First interesting result was that P20/N20, P60/N60 and P100/N100 constituted distinct clusters which further supports that early and late components were not linked. Second, we found four clusters in both MEG and EEG. At the latency of P20/N20, we found common MEG and EEG activities in SI, M1, SMG and PM as the most representative variables in the cluster. Regarding P60/N60, we found one cluster in MEG and two in EEG. The common cluster included SI, M1, PM and SII and the second cluster in EEG included associative cortices (iPPC, sPPC, SMG and STS). Lastly, at the latency of P100/N100, we found one common cluster involving SI, M1, SMG and PCC; the second cluster only observed in MEG included STS and insula. These results indicate that MEG/EEG main activity was commonly observed in SI and M1 during early and late SEPs without any link between components. The three components were distinct by activity in PM during P20/N20 and P60/N60, and SII has particularly contributed to P60/N60 and PCC to P100/N100.

## 4 | DISCUSSION

This first aim of the study was to investigate the temporality of cortical activation maps after median nerve stimulation at the wrist level. It is shown that the contralateral primary sensorimotor area (SI-M1) in the central sulcus is first activated (18 ms) and rapidly, still during the time window covering P20/N20, activity in contralateral SMG, PM, SII and both contralateral and ipsilateral PCC has occurred. At longer latency (>30 ms) and during P60/N60 and P100/N100, activity in these areas was combined to activity in contralateral

multisensory associative cortices (sPPC, iPPC, STS and insula) and SMA and in ipsilateral SII.

The second aim was to investigate the relationship between stimulus intensity and source activities in the different ROIs to further identify specific features of late SEPs as compared with P20/N20. The first interesting finding included similar results in MEG and EEG during P20/N20 but not during late SEPs. Furthermore, while all responses plateaued at intensity between three and six times the PT, the relationship between stimulus intensity and late responses was similar but different from P20/N20. Lastly, correlation and cluster analyses did not reveal any significant link between early and late components. However, clustered activity in the primary sensorimotor area (SI-M1) was consistently observed during the early and late components, each one being characterised by added activity in PM and SMG during P20/N20, in SII and PM during P60/N60 and in SMG and PCC during P100/N100. Late SEPs were also characterised by another cluster including multisensory associative cortices (iPPC, sPPC, SMG, STS and insula).

### 4.1 | Extra-somatosensory activity during P20/N20

It has been well established that P20/N20 is generated in the contralateral primary somatosensory cortex, particularly in areas 3b and 1, in response to cutaneous inputs from median nerve stimulation (Allison et al., 1991; Baumgärtner et al., 2010; Hashimoto et al., 2001; Mauguiere, 2005; Papadelis et al., 2011; Valeriani et al., 2001). Studies using source imaging have consistently revealed that cortical activity is maximal in the central sulcus (Antonakakis et al., 2019; Rezaei et al., 2021). In the present study, maximal activity was also found in the central sulcus at 20 ms (Video S1). However, to a smaller extent but statistically significant, activity in pre- and post-central sulci was generated at the same time.

P20/N20 activity was quantified in ROIs defined according to Desikan-Killiany and Brodmann atlases projected onto individual MRIs, within a time window covering the full duration of the component (16–22 ms), while in most studies, peak activity (~20 ms) was used to quantify the cortical activity. Time-window analysis (instead of peak activity) was chosen to enable reliable comparison between early and late components because the latter are characterized by slow signal with peak activity extremely variable from one individual to another (see Figure 2a,b). On one hand, calculating activity within the full-time window increases the signal-to-noise ratio and enables a better extraction of stimulus-

induced cortical activity from background activity and noise. On the other hand, it takes into account a broader activity, possibly exceeding that in area 3b characterised at the peak activity. However, this is unlikely because cortical activity at the peak latency for N20 and P22 has been, respectively, localised in area 3b and area 1 (Baumgärtner et al., 2010; Hashimoto et al., 2001; Mauguiere, 2005; Papadelis et al., 2011), and here, we found that activity in the pre-, post- and central sulci was generated simultaneously.

ROIs and statistical analyses revealed that P20/N20 was characterised by activity in SI, M1, PM and SMG (the two later ROIs being likely associated to activity in pre- and post-central sulci, respectively). Importantly, results in MEG and EEG were similar. EEG is indeed sensitive to both tangential and radial dipoles, while MEG is less sensitive but not fully blind to radial sources (Leahy et al., 1998). Accordingly, a possible greater localisation error in EEG, compared with MEG, is still a matter of debate, being between 3 mm and 1.5 cm according to the authors (Baillet, 2017; Komssi et al., 2004; Leahy et al., 1998). However, the error in EEG is reduced when using high-density EEG (32 to 256 electrodes; error decreasing when using more than 32 electrodes), individual MRI for more precise information of head anatomy and sophisticated source localisation algorithms (Baillet et al., 2001; Komssi et al., 2004; Michel et al., 2004; Michel & Brunet, 2019; Michel & He, 2019; Michel & Murray, 2012).

The central sulcus includes part of M1 (anterior bank) and areas 3a and 3b of SI (posterior bank); its deep part being a combination of both M1 and area 3a. It has been established that P20/N20 is generated in the posterior bank of the central sulcus corresponding to area 3b (Allison et al., 1991) but variations in central sulcus anatomy may cause unusual SEP topographies (Legatt & Kader, 2000) and likely the high interindividual variability, thus limiting the precise location of source activity. While M1 and SI ROIs did not overlap (pre- and post-central gyri, respectively; sparing the deep part of the central sulcus), our approach does not allow to determine whether activity in M1 during P20/N20 was real or due to diffusion of activity generated in area 3b (Schoffelen & Gross, 2009). Alternatively, one would argue that the activation of M1 could be related to the activation of motor axons at the peripheral nerve level, but this is unlikely because (i) the antidromic volley in motor axons is limited to spinal motoneurons and could only induce proprioceptive afferent inputs in response to muscle twitch, in addition to the direct electrical volley in sensory afferents (Pierrot-Deseilligny & Burke, 2005), and (ii) we found activity in M1 even at 1.5 times the PT, that is, below MT. Moreover, activity in precentral gyrus was clearly observed from

30 ms (Video S1) and the close link between SI and M1 activities was systematically observed during the three components while activity during the three components was not correlated. This suggests that the activity quantified in M1 ROI was likely not of the same origin from one component to another nor that, in SI given, the temporality of activity changes in both ROIs.

Can we argue that P20/N20 activity was only limited to area 3b? Several lines of evidence do not fully support this assumption. First, we cannot fully discard a contribution of M1 because it has been shown to be activated during P20/N20 in animal models (Lemon, 1981; Peterson et al., 1995; Tanji & Wise, 1981) and transcranial magnetic stimulation in humans has revealed that SI and M1 are comodulated by somatosensory inputs (Schabrun et al., 2012). Moreover, high-frequency oscillations during P20/N20 are partly due to presynaptic activity in thalamo-cortical projections (Gobbelé et al., 2003, 2004; Jaros et al., 2008; Sakura et al., 2009; Urasaki et al., 2002) which is further supported by subcortical source analysis which revealed the contribution of the lateral ventro-parietal nuclei of the thalamus (relay of the somatosensory afferents to SI and SII; Rezaei et al., 2021). Lastly, we found activity in pre- and post-central sulci likely associated to activity in premotor areas (PM) and associative cortex (SMG).

## 4.2 | Characteristics of late components

Late components were characterised by different clusters than those identified during P20/N20 which is consistent with the absence of correlation between the three components, especially between P20/N20 and P60/N60, and the fact that I/O relationships were different between early and late components. The late components have been studied to a much smaller extent compared with P20/N20, and little is known on their origin and they are not used in clinical routine. To date, the knowledge is limited to the implication of contralateral SII, which is thus considered as the region of late cortical responses to peripheral nerve stimuli (Mauguiere, 2005). Source imaging in the present study has revealed a much broader cortical activity during late components, involving a more complex cortico-cortical sensorimotor network. Moreover, we found significant activity in the ipsilateral SII using both MEG and EEG, as previously reported using intracerebral recordings which has been attributed to deep source (Barba et al., 2002; Mauguiere, 2005).

Besides the location of dipoles or magnetic fields, several studies aimed at investigating the influence of stimulus intensity on SI/SII activity or P20/N20–P60/N60

strength (I/O relationship), to compare the characteristics of early and late responses. All studies reported a plateaued effect affecting SI/P20/N20 only (Gerber & Meinck, 2000; Torquati et al., 2002) or both SI/P20/N20 and SII/P60/N60 (Huttunen, 1995; Lin et al., 2003) or only SII response (Jousmäki & Forss, 1998). Because the stimulus intensity was not normalised or normalised but not the same way from one study to another and even in the same study, it is difficult to determine exactly the minimum intensity for saturation but plateau was reported between two and three times the PT and one times MT. In the present study, intensity was normalised to PT (Fukuda et al., 2007) and we investigated the I/O relationship taking into account the different ROIs. First of all, we found that the main increase occurred between 1.5 and 3 times the PT, which was more marked for EEG than for MEG. Plateau effect was much clearer for P20/N20 than for late components, occurring between three and six times the PT (Figure 5b,c). We did not check MT in our experimental group, but in previous studies in our laboratory, we found that MT in median nerve is about four times the PT, ranging from three to six times the PT. Therefore, plateaued effect manifested at intensity greater than or equal to one times the MT, as previously reported for P20/N20. This was true in almost all areas with less difference between Z-scores at intensity greater than or equal to six times the PT in MEG and greater than or equal to three times the PT in EEG (Figure 6a,b), except SII whose response decreased with intensity greater than six times the PT. Similar decrease in SII response with stimulus intensity has already been reported but without specifying the timing (Torquati et al., 2002). In line with the fact that saturation was observed mainly during P20/N20, as reported previously (Gerber & Meinck, 2000; Huttunen, 1995; Lin et al., 2003; Torquati et al., 2002), we found similar I/O relationship for P60/N60 and P100/N100 but different for P20/N20. Indeed, both P60/N60 and P100/N100 mostly still increased with stimulus intensity greater than three times the PT but with slower slope than between 1.5 and 3 times the PT (Figure 5c,d). The fact that we did not observe a clear plateau effect is not contradictory from previous studies given the great variability of SEP responses (Huttunen, 1995; Jousmäki & Forss, 1998; Lin et al., 2003).

Five clusters of ROIs but different from one component to another could be identified. We consistently found SI and M1 in one cluster for each component, which might be due to leakage activity between these two very close areas (Schoffelen & Gross, 2009). However, because there was no correlation between components, there is a possibility that activity in these two ROIs is not of the same origin from one component to another

(activity mostly in central sulcus during P20/N20, *plus* enhanced activity in pre- and post-central gyri at latency  $\geq 30$  ms). Moreover, the cluster including SI–M1 involves other areas as main variables but different from one component to another: PM and SMG during P20/N20, SII and PM during P60/N60 and SMG and PCC during P100/N100. The two other clusters involved multisensory associative cortex with iPPC, sPPC, SMG and STS during P60/N60 and STS and insula during P100/N100. These results suggest that late components are likely not characterised by activity in SII only but might involve more complex cortico-cortical interactions, including the primary and secondary somatosensory areas, motor, premotor and multisensory associative cortices in the contralateral hemisphere and ipsilateral SII.

### 4.3 | Cortical network(s) underlying late SEPs and functional implications

EEG and MEG source imaging has revealed a much broader activity at cortical level than reported previously, both during early and late SEPs. While it is globally admitted that P20/N20 is limited to activity of area 3b neurons, the present study has revealed activity in pre- and post-central sulci likely linked to activity in PM and SMG ROIs. Similarly, late components are not limited to activity in SII but are the result of activity in the same areas as during P20/N20, *plus* SII (both hemispheres) and multisensory associative cortices (iPPC, sPPC, STS, PCC and insula). While the time resolution of functional MRI does not allow to distinguish activity between early and late components, the mapping of hemodynamic responses after electrical median nerve stimulation and mechanical stimulation of hand skin (Boakye et al., 2000) fully matches the present results of EEG/MEG source imaging.

Besides different source locations, early and late components exhibited different sensitivity to stimulus intensity, suggesting the contribution of different neural networks with distinct I/O relationships. Brain connectivity has been assessed after median nerve stimulation but the studies focussed on SI, SI–M1 or the resulting change in default mode and fronto-parietal networks has been studied (Kobayashi et al., 2015; Mayhew et al., 2014; Porcaro et al., 2013; Tecchio et al., 2005). Further studies need to be undertaken to evaluate the dynamical functional connectivity between brain areas activated by median nerve stimulation we reported here, and previously using fMRI (Boakye et al., 2000), specifically in the different clusters of activity we identified. Such investigations would also help to (i) establish whether SII receive a copy of afferent inputs through direct thalamocortical

projections and/or indirectly via SI and (ii) elucidate the roles of these two areas in somatosensory processing at the cortical level (Klingner et al., 2016; Mauguiere, 2005). If both areas were involved in the same network, one would expect the activity in both areas would be correlated to some extent, which is not supported by the present study.

It is well established that SI is the first and main target of thalamocortical projections relaying peripheral afferent inputs to cerebral cortex and M1, the main cortical output in motor system; the interaction between both being mediated through associative cortex and sPPC in particular (Coquery, 2011). Both sPPC and iPPC receive multimodal sensory inputs and are involved in sensorimotor control (feedback control), recognition, motor planning, executive and working memory and motor learning (Binkofski & Buccino, 2018; Buneo & Andersen, 2006; Mesulam, 1998; Tumati et al., 2019). Lastly, premotor areas, including SMA and PM, are involved in condition–action association, motor planning, initiation and learning (Binkofski & Buccino, 2006; Davare et al., 2006; Nachev et al., 2008; Rizzolatti & Craighero, 2004; Solopchuk et al., 2016). All these areas take part in several neural networks involved in the integration of sensory information to initiate multiple cognitive and behavioural outcomes (Mesulam, 1998), which supports the results of EEG/MEG source imaging in the present study. However, the identification of brain areas activated by somatosensory inputs is not sufficient to understand how those inputs are processed at cortical level during motor and cognitive functions. This also requires a better knowledge of their interactions and, particularly, the pathways by which sensory information is mediated.

#### 4.4 | Impacts for future studies and clinical investigations

It is commonly accepted that somatosensory inputs to the cortex undergo early and late stages of processing. This way, early and late SEPs have been often compared to better evaluate the influence of somatosensory inputs and their gating in the different phases of movement (planning, initiation and execution; Mouchnino et al., 2017; Saradjian et al., 2013). Although elegant and particularly ingenious, this approach gives rise to results that should be considered with caution given the great overlap in the brain areas involved in early and late SEPs and their possible interaction. In line with this, in our previous study in patients with ALS (Sangari et al., 2016), we found that late SEPs were more altered than early SEPs, and their alteration was not correlated. The present

results further confirm that early and late SEPs reflect activity in different neural networks involving sensorimotor and nonmotor areas and that their correlation, if anything, is low. However, the comparison between early and late SEPs, during specific tasks and in pathological conditions, should be performed using high-density EEG allowing source imaging for accurate evaluation of brain processing.

## 5 | CONCLUSIONS

The present study revisits the origin of late SEPs. The focus was on P60/N60 and P100/N100 that we compared with a priori well-known P20/N20 component. Further investigations would be interesting to better understand the dynamics of brain processing, including intermediate components of SEPs; something solely possible using EEG/MEG source imaging which finally was only few used to investigate the early and late phases of brain processing of somatosensory inputs, to date. In addition, this study indicates that the clinical use of SEPs is particularly limited given the potential information on brain functions such an approach can give, not only on the transmission along the sensory pathway. Further research on signal processing, comparing the results of clinical SEP investigation in routine (with simple setup) and complex laboratory EEG/MEG source imaging (difficult to implement in routine), would be particularly interesting to evaluate the respective role of the different networks underlying early and late SEPs, in order to propose new biomarkers of brain functions and complex processing, that would enable to implement the use of late SEPs in clinics, to evaluate brain functions in patients.

### AUTHOR CONTRIBUTIONS

**Sahar Hssain-Khalladi:** Investigation; Formal analysis; Writing – original draft. **Alain Giron:** Formal analysis. **Clément Huneau:** Supervision; Formal analysis. **Christophe Gitton:** Investigation-. **Denis Schwartz:** Conceptualization; Methodology; Supervision; Formal analysis; Validation. **Nathalie George:** Conceptualization; Methodology; Supervision; Validation. **Michel Le Van Quyen:** Supervision; Validation. **Guillaume Marrelec:** Methodology; Writing – review & editing. **Véronique Marchand-Pauvert:** Conceptualization; Methodology; Investigation; Formal analysis; Writing – review & editing.

### ACKNOWLEDGEMENTS

This work was supported by annual financial support of Inserm, Sorbonne Université and CNRS. S. Hssain-Khalladi was a PhD student (supervised by V. Marchand-

Pauvert) funded by a grant from LabEX SMART (Sorbonne Université) which was supported by French State funds managed by *Agence Nationale de la Recherche* (ANR) within the *Programme Investissements d'Avenir* (PIA; ID: ANR-11-IDEX-0004-02). The authors thank all the participants.

### CONFLICT OF INTEREST STATEMENT

None of the authors have potential conflicts of interest to be disclosed.

### PEER REVIEW

The peer review history for this article is available at <https://www.webofscience.com/api/gateway/wos/peer-review/10.1111/ejn.16379>.

### DATA AVAILABILITY STATEMENT

The data that support the findings of this study are available on request from N. G. among the authors; they are not publicly available due to ethical restrictions.

### ORCID

Véronique Marchand-Pauvert  <https://orcid.org/0000-0002-0226-7169>

### REFERENCES

- Ahn, S., Kim, K., & Jun, S. C. (2015). Steady-state somatosensory evoked potential for brain-computer interface—Present and future. *Frontiers in Human Neuroscience*, *9*, 716. <https://doi.org/10.3389/fnhum.2015.00716>
- Allison, T., McCarthy, G., Wood, C. C., & Jones, S. J. (1991). Potentials evoked in human and monkey cerebral cortex by stimulation of the median nerve. A review of scalp and intracranial recordings. *Brain*, *114*(Pt 6), 2465–2503. <https://doi.org/10.1093/brain/114.6.2465>
- Antonakakis, M., Schrader, S., Wollbrink, A., Oostenveld, R., Rapp, S., Hauelsen, J., & Wolters, C. H. (2019). The effect of stimulation type, head modeling, and combined EEG and MEG on the source reconstruction of the somatosensory P20/N20 component. *Human Brain Mapping*, *40*, 5011–5028. <https://doi.org/10.1002/hbm.24754>
- Baillet, S. (2017). Magnetoencephalography for brain electrophysiology and imaging. *Nature Neuroscience*, *20*, 327–339. <https://doi.org/10.1038/nn.4504>
- Baillet, S., Garnero, L., Marin, G., & Hugonin, J. P. (1999). Combined MEG and EEG source imaging by minimization of mutual information. *IEEE Transactions on Biomedical Engineering*, *46*, 522–534. <https://doi.org/10.1109/10.759053>
- Baillet, S., Riera, J. J., Marin, G., Mangin, J. F., Aubert, J., & Garnero, L. (2001). Evaluation of inverse methods and head models for EEG source localization using a human skull phantom. *Physics in Medicine and Biology*, *46*, 77–96. <https://doi.org/10.1088/0031-9155/46/1/306>
- Barba, C., Frot, M., Valeriani, M., Tonali, P., & Mauguière, F. (2002). Distinct fronto-central N60 and supra-sylvian N70 middle-latency components of the median nerve SEPs as assessed by scalp topographic analysis, dipolar source modeling and depth recordings. *Clinical Neurophysiology*, *113*, 981–992. [https://doi.org/10.1016/S1388-2457\(02\)00104-9](https://doi.org/10.1016/S1388-2457(02)00104-9)
- Baumgärtner, U., Vogel, H., Ohara, S., Treede, R.-D., & Lenz, F. A. (2010). Dipole source analyses of early median nerve SEP components obtained from subdural grid recordings. *Journal of Neurophysiology*, *104*, 3029–3041. <https://doi.org/10.1152/jn.00116.2010>
- Binkofski, F., & Buccino, G. (2006). The role of ventral premotor cortex in action execution and action understanding. *Journal of Physiology, Paris*, *99*, 396–405. <https://doi.org/10.1016/j.jphysparis.2006.03.005>
- Binkofski, F., & Buccino, G. (2018). The role of the parietal cortex in sensorimotor transformations and action coding. *Handbook of Clinical Neurology*, *151*, 467–479. <https://doi.org/10.1016/B978-0-444-63622-5.00024-3>
- Boakye, M., Huckins, S. C., Szeverenyi, N. M., Taskey, B. I., & Hodge, C. J. (2000). Functional magnetic resonance imaging of somatosensory cortex activity produced by electrical stimulation of the median nerve or tactile stimulation of the index finger. *Journal of Neurosurgery*, *93*, 774–783. <https://doi.org/10.3171/jns.2000.93.5.0774>
- Buchner, H., Adams, L., Müller, A., Ludwig, I., Knepper, A., Thron, A., Niemann, K., & Scherg, M. (1995). Somatotopy of human hand somatosensory cortex revealed by dipole source analysis of early somatosensory evoked potentials and 3D-NMR tomography. *Electroencephalography and Clinical Neurophysiology*, *96*, 121–134. [https://doi.org/10.1016/0168-5597\(94\)00228-7](https://doi.org/10.1016/0168-5597(94)00228-7)
- Buchner, H., Fuchs, M., Wischmann, H. A., Dössel, O., Ludwig, I., Knepper, A., & Berg, P. (1994). Source analysis of median nerve and finger stimulated somatosensory evoked potentials: Multichannel simultaneous recording of electric and magnetic fields combined with 3D-MR tomography. *Brain Topography*, *6*, 299–310. <https://doi.org/10.1007/BF01211175>
- Buneo, C. A., & Andersen, R. A. (2006). The posterior parietal cortex: Sensorimotor interface for the planning and online control of visually guided movements. *Neuropsychologia*, *44*, 2594–2606. <https://doi.org/10.1016/j.neuropsychologia.2005.10.011>
- Coquery, J. (2011). *Neurosciences: Purves, Augustine, Hall, Laman-tia, MacNamara, Willimans* (4e ed.). Neurosciences et Cognition. de Boeck, Bruxelles.
- Davare, M., Andres, M., Cosnard, G., Thonnard, J.-L., & Olivier, E. (2006). Dissociating the role of ventral and dorsal premotor cortex in precision grasping. *The Journal of Neuroscience*, *26*, 2260–2268. <https://doi.org/10.1523/JNEUROSCI.3386-05.2006>
- Desmedt, J. E., & Cheron, G. (1980). Somatosensory evoked potentials to finger stimulation in healthy octogenarians and in young adults: Wave forms, scalp topography and transit times of parietal and frontal components. *Electroencephalography and Clinical Neurophysiology*, *50*, 404–425. [https://doi.org/10.1016/0013-4694\(80\)90007-3](https://doi.org/10.1016/0013-4694(80)90007-3)
- Desmedt, J. E., & Cheron, G. (1981). Non-cephalic reference recording of early somatosensory potentials to finger stimulation in adult or aging normal man: Differentiation of widespread N18 and contralateral N20 from the prerolandic P22 and N30 components. *Electroencephalography and Clinical Neurophysiology*, *52*, 553–570. [https://doi.org/10.1016/0013-4694\(81\)91430-9](https://doi.org/10.1016/0013-4694(81)91430-9)

- Forss, N., Jousmäki, V., & Hari, R. (1995). Interaction between afferent input from fingers in human somatosensory cortex. *Brain Research*, 685, 68–76. [https://doi.org/10.1016/0006-8993\(95\)00424-0](https://doi.org/10.1016/0006-8993(95)00424-0)
- Fukuda, H., Sonoo, M., Kako, M., & Shimizu, T. (2007). Optimal method to determine the stimulus intensity for median nerve somatosensory evoked potentials. *Journal of Clinical Neurophysiology*, 24, 358–362.
- Gerber, J., & Meinck, H. M. (2000). The effect of changing stimulus intensities on median nerve somatosensory-evoked potentials. *Electromyography and Clinical Neurophysiology*, 40, 477–482.
- Gobbelé, R., Waberski, T. D., Simon, H., Peters, E., Klostermann, F., Curio, G., & Buchner, H. (2004). Different origins of low- and high-frequency components (600 Hz) of human somatosensory evoked potentials. *Clinical Neurophysiology*, 115, 927–937. <https://doi.org/10.1016/j.clinph.2003.11.009>
- Gobbelé, R., Waberski, T. D., Thyerlei, D., Thissen, M., Darvas, F., Klostermann, F., Curio, G., & Buchner, H. (2003). Functional dissociation of a subcortical and cortical component of high-frequency oscillations in human somatosensory evoked potentials by motor interference. *Neuroscience Letters*, 350, 97–100. [https://doi.org/10.1016/S0304-3940\(03\)00877-2](https://doi.org/10.1016/S0304-3940(03)00877-2)
- Gramfort, A., Papadopoulos, T., Olivi, E., & Clerc, M. (2010). Open-MEEG: Opensource software for quasistatic bioelectromagnetics. *Biomedical Engineering Online*, 9, 45. <https://doi.org/10.1186/1475-925X-9-45>
- Hagiwara, K., Ogata, K., Okamoto, T., Uehara, T., Hironaga, N., Shigeto, H., Kira, J., & Tobimatsu, S. (2014). Age-related changes across the primary and secondary somatosensory areas: An analysis of neuromagnetic oscillatory activities. *Clinical Neurophysiology: Official Journal of the International Federation of Clinical Neurophysiology*, 125, 1021–1029. <https://doi.org/10.1016/j.clinph.2013.10.005>
- Hämäläinen, M. S., & Ilmoniemi, R. J. (1994). Interpreting magnetic fields of the brain: Minimum norm estimates. *Medical & Biological Engineering & Computing*, 32, 35–42. <https://doi.org/10.1007/BF02512476>
- Hashimoto, I., Kimura, T., Iguchi, Y., Takino, R., & Sekihara, K. (2001). Dynamic activation of distinct cytoarchitectonic areas of the human SI cortex after median nerve stimulation. *Neuroreport*, 12, 1891–1897. <https://doi.org/10.1097/00001756-200107030-00025>
- Huang, M.-X., Song, T., Hagler, D. J., Podgorny, I., Jousmaki, V., Cui, L., Gaa, K., Harrington, D. L., Dale, A. M., Lee, R. R., Elman, J., & Halgren, E. (2007). A novel integrated MEG and EEG analysis method for dipolar sources. *NeuroImage*, 37, 731–748. <https://doi.org/10.1016/j.neuroimage.2007.06.002>
- Huttunen, J. (1995). Effects of stimulus intensity on frontal, central and parietal somatosensory evoked potentials after median nerve stimulation. *Electromyography and Clinical Neurophysiology*, 35, 217–223.
- Huttunen, J., Wikström, H., Salonen, O., & Ilmoniemi, R. J. (1999). Human somatosensory cortical activation strengths: Comparison between males and females and age-related changes. *Brain Research*, 818, 196–203. [https://doi.org/10.1016/S0006-8993\(98\)01215-3](https://doi.org/10.1016/S0006-8993(98)01215-3)
- Jaros, U., Hilgenfeld, B., Lau, S., Curio, G., & Haueisen, J. (2008). Nonlinear interactions of high-frequency oscillations in the human somatosensory system. *Clinical Neurophysiology*, 119, 2647–2657. <https://doi.org/10.1016/j.clinph.2008.08.011>
- Jousmäki, V., & Forss, N. (1998). Effects of stimulus intensity on signals from human somatosensory cortices. *Neuroreport*, 9, 3427–3431. <https://doi.org/10.1097/00001756-199810260-00017>
- Kakigi, R., & Shibasaki, H. (1991). Effects of age, gender, and stimulus side on scalp topography of somatosensory evoked potentials following median nerve stimulation. *Journal of Clinical Neurophysiology: Official Publication of the American Electroencephalographic Society*, 8, 320–330. <https://doi.org/10.1097/00004691-199107010-00008>
- Klingner, C. M., Brodoehl, S., Huonker, R., & Witte, O. W. (2016). The processing of somatosensory information shifts from an early parallel into a serial processing mode: A combined fMRI/MEG study. *Frontiers in Systems Neuroscience*, 10, 103. <https://doi.org/10.3389/fnsys.2016.00103>
- Kobayashi, K., Matsumoto, R., Matsushashi, M., Usami, K., Shimotake, A., Kunieda, T., Kikuchi, T., Mikuni, N., Miyamoto, S., Fukuyama, H., Takahashi, R., & Ikeda, A. (2015). Different mode of afferents determines the frequency range of high frequency activities in the human brain: Direct electrocorticographic comparison between peripheral nerve and direct cortical stimulation. *PLoS ONE*, 10, e0130461. <https://doi.org/10.1371/journal.pone.0130461>
- Komssi, S., Huttunen, J., Aronen, H. J., & Ilmoniemi, R. J. (2004). EEG minimum-norm estimation compared with MEG dipole fitting in the localization of somatosensory sources at S1. *Clinical Neurophysiology*, 115, 534–542. <https://doi.org/10.1016/j.clinph.2003.10.034>
- Kybic, J., Clerc, M., Abboud, T., Faugeras, O., Keriven, R., & Papadopoulos, T. (2005). A common formalism for the integral formulations of the forward EEG problem. *IEEE Transactions on Medical Imaging*, 24, 12–28. <https://doi.org/10.1109/TMI.2004.837363>
- Lanfer, B., Scherg, M., Dannhauer, M., Knösche, T. R., Burger, M., & Wolters, C. H. (2012). Influences of skull segmentation inaccuracies on EEG source analysis. *NeuroImage*, 62, 418–431. <https://doi.org/10.1016/j.neuroimage.2012.05.006>
- Leahy, R. M., Mosher, J. C., Spencer, M. E., Huang, M. X., & Lewine, J. D. (1998). A study of dipole localization accuracy for MEG and EEG using a human skull phantom. *Electroencephalography and Clinical Neurophysiology*, 107, 159–173. [https://doi.org/10.1016/S0013-4694\(98\)00057-1](https://doi.org/10.1016/S0013-4694(98)00057-1)
- Legatt, A. D., & Kader, A. (2000). Topography of the initial cortical component of the median nerve somatosensory evoked potential. Relationship to central sulcus anatomy. *Journal of Clinical Neurophysiology*, 17, 321–325. <https://doi.org/10.1097/00004691-200005000-00009>
- Lemon, R. N. (1981). Functional properties of monkey motor cortex neurones receiving afferent input from the hand and fingers. *The Journal of Physiology*, 311, 497–519. <https://doi.org/10.1113/jphysiol.1981.sp013601>
- Lin, Y.-Y., Shih, Y.-H., Chen, J.-T., Hsieh, J.-C., Yeh, T.-C., Liao, K.-K., Kao, C.-D., Lin, K.-P., Wu, Z.-A., & Ho, L.-T. (2003). Differential effects of stimulus intensity on peripheral and neuromagnetic cortical responses to median nerve stimulation. *NeuroImage*, 20, 909–917. [https://doi.org/10.1016/S1053-8119\(03\)00387-2](https://doi.org/10.1016/S1053-8119(03)00387-2)
- Mauguiere, F. (2005). Somatosensory evoked potentials: normal responses, abnormal waveforms, and clinical applications in neurological disease. In E. Niedermeyer & F. Lopes da Silva (Eds.), *Electroencephalography. Basic principles, clinical*

- applications, and related fields* (pp. 1067–1119). Lippincott, Williams & Wilkins, Philadelphia.
- Mauguière, F., Merlet, I., Forss, N., Vanni, S., Jousmäki, V., Adeleine, P., & Hari, R. (1997). Activation of a distributed somatosensory cortical network in the human brain: A dipole modelling study of magnetic fields evoked by median nerve stimulation. Part II: Effects of stimulus rate, attention and stimulus detection. *Electroencephalography and Clinical Neurophysiology/Evoked Potentials Section*, *104*, 290–295. [https://doi.org/10.1016/S0013-4694\(97\)00018-7](https://doi.org/10.1016/S0013-4694(97)00018-7)
- Mayhew, S. D., Mullinger, K. J., Bagshaw, A. P., Bowtell, R., & Francis, S. T. (2014). Investigating intrinsic connectivity networks using simultaneous BOLD and CBF measurements. *NeuroImage*, *99*, 111–121. <https://doi.org/10.1016/j.neuroimage.2014.05.042>
- Mesulam, M. M. (1998). From sensation to cognition. *Brain*, *121*(Pt 6), 1013–1052. <https://doi.org/10.1093/brain/121.6.1013>
- Michel, C. M., & Brunet, D. (2019). EEG source imaging: A practical review of the analysis steps. *Frontiers in Neurology*, *10*, 325. <https://doi.org/10.3389/fneur.2019.00325>
- Michel, C. M., & He, B. (2019). EEG source localization. *Handbook of Clinical Neurology*, *160*, 85–101. <https://doi.org/10.1016/B978-0-444-64032-1.00006-0>
- Michel, C. M., & Murray, M. M. (2012). Towards the utilization of EEG as a brain imaging tool. *NeuroImage*, *61*, 371–385. <https://doi.org/10.1016/j.neuroimage.2011.12.039>
- Michel, C. M., Murray, M. M., Lantz, G., Gonzalez, S., Spinelli, L., & Grave de Peralta, R. (2004). EEG source imaging. *Clinical Neurophysiology*, *115*, 2195–2222. <https://doi.org/10.1016/j.clinph.2004.06.001>
- Mideksa, K. G., Hellriegel, H., Hoogenboom, N., Krause, H., Schnitzler, A., Deuschl, G., Raethjen, J., Heute, U., & Muthuraman, M. (2012). Source analysis of median nerve stimulated somatosensory evoked potentials and fields using simultaneously measured EEG and MEG signals. *Conference Proceedings: Annual International Conference of the IEEE Engineering in Medicine and Biology Society, 2012*, 4903–4906.
- Morizot-Koutlidis, R., André-Obadia, N., Antoine, J.-C., Attarian, S., Ayache, S. S., Azabou, E., Benaderette, S., Camdessanché, J.-P., Cassereau, J., Convers, P., d'Anglejean, J., Delval, A., Durand, M.-C., Etard, O., Fayet, G., Fournier, E., Franques, J., Gavaret, M., Guehl, D., ... Lefaucheur, J.-P. (2015). Somatosensory evoked potentials in the assessment of peripheral neuropathies: Commented results of a survey among French-speaking practitioners and recommendations for practice. *Neurophysiologie Clinique*, *45*, 131–142. <https://doi.org/10.1016/j.neucli.2015.04.001>
- Mouchnino, L., Lhomond, O., Morant, C., & Chavet, P. (2017). Plantar sole unweighting alters the sensory transmission to the cortical areas. *Frontiers in Human Neuroscience*, *11*, 220. <https://doi.org/10.3389/fnhum.2017.00220>
- Nachev, P., Kennard, C., & Husain, M. (2008). Functional role of the supplementary and pre-supplementary motor areas. *Nature Reviews. Neuroscience*, *9*, 856–869. <https://doi.org/10.1038/nrn2478>
- Nakamura, A., Yamada, T., Goto, A., Kato, T., Ito, K., Abe, Y., Kachi, T., & Kakigi, R. (1998). Somatosensory homunculus as drawn by MEG. *NeuroImage*, *7*, 377–386. <https://doi.org/10.1006/nimg.1998.0332>
- Oldfield, R. C. (1971). The assessment and analysis of handedness: The Edinburgh inventory. *Neuropsychologia*, *9*, 97–113. [https://doi.org/10.1016/0028-3932\(71\)90067-4](https://doi.org/10.1016/0028-3932(71)90067-4)
- Onishi, H., Sugawara, K., Yamashiro, K., Sato, D., Suzuki, M., Kirimoto, H., Tamaki, H., Murakami, H., & Kameyama, S. (2013). Effect of the number of pins and inter-pin distance on somatosensory evoked magnetic fields following mechanical tactile stimulation. *Brain Research*, *1535*, 78–88. <https://doi.org/10.1016/j.brainres.2013.08.048>
- Papadelis, C., Eickhoff, S. B., Zilles, K., & Ioannides, A. A. (2011). BA3b and BA1 activate in a serial fashion after median nerve stimulation: Direct evidence from combining source analysis of evoked fields and cytoarchitectonic probabilistic maps. *NeuroImage*, *54*, 60–73. <https://doi.org/10.1016/j.neuroimage.2010.07.054>
- Passmore, S. R., Murphy, B., & Lee, T. D. (2014). The origin, and application of somatosensory evoked potentials as a neurophysiological technique to investigate neuroplasticity. *J Can Chiropr Assoc*, *58*, 170–183.
- Peterson, N. N., Schroeder, C. E., & Arezzo, J. C. (1995). Neural generators of early cortical somatosensory evoked potentials in the awake monkey. *Electroencephalography and Clinical Neurophysiology*, *96*, 248–260. [https://doi.org/10.1016/0168-5597\(95\)00006-E](https://doi.org/10.1016/0168-5597(95)00006-E)
- Pierrot-Deseilligny, E., & Burke, D. (2005). *The circuitry of the human spinal cord*. Cambridge University Press. <https://doi.org/10.1017/CBO9780511545047>
- Porcaro, C., Coppola, G., Pierelli, F., Seri, S., Di Lorenzo, G., Tomasevic, L., Salustri, C., & Tecchio, F. (2013). Multiple frequency functional connectivity in the hand somatosensory network: An EEG study. *Clinical Neurophysiology*, *124*, 1216–1224. <https://doi.org/10.1016/j.clinph.2012.12.004>
- Pratt, H., Politoske, D., & Starr, A. (1980). Mechanically and electrically evoked somatosensory potentials in humans: Effects of stimulus presentation rate. *Electroencephalography and Clinical Neurophysiology*, *49*, 240–249. [https://doi.org/10.1016/0013-4694\(80\)90218-7](https://doi.org/10.1016/0013-4694(80)90218-7)
- Rezaei, A., Lahtinen, J., Neugebauer, F., Antonakakis, M., Piastra, M. C., Koulouri, A., Wolters, C. H., & Pursiainen, S. (2021). Reconstructing subcortical and cortical somatosensory activity via the RAMUS inverse source analysis technique using median nerve SEP data. *NeuroImage*, *245*, 118726. <https://doi.org/10.1016/j.neuroimage.2021.118726>
- Rizzolatti, G., & Craighero, L. (2004). The mirror-neuron system. *Annual Review of Neuroscience*, *27*, 169–192. <https://doi.org/10.1146/annurev.neuro.27.070203.144230>
- Sakura, Y., Terada, K., Usui, K., Baba, K., Usui, N., Umeoka, S., Yamaguchi, M., Matsuda, K., Tottori, T., Mihara, T., Nakamura, F., & Inoue, Y. (2009). Very high-frequency oscillations (over 1000 Hz) of somatosensory-evoked potentials directly recorded from the human brain. *Journal of Clinical Neurophysiology*, *26*, 414–421. <https://doi.org/10.1097/WNP.0b013e3181c298c9>
- Sangari, S., Iglesias, C., El Mendili, M.-M., Benali, H., Pradat, P.-F., & Marchand-Pauvert, V. (2016). Impairment of sensory-motor integration at spinal level in amyotrophic lateral sclerosis. *Clinical Neurophysiology*, *127*, 1968–1977. <https://doi.org/10.1016/j.clinph.2016.01.014>
- Saradjian, A. H., Tremblay, L., Perrier, J., Blouin, J., & Mouchnino, L. (2013). Cortical facilitation of proprioceptive

- inputs related to gravitational balance constraints during step preparation. *Journal of Neurophysiology*, *110*, 397–407. <https://doi.org/10.1152/jn.00905.2012>
- Schabrun, S. M., Ridding, M. C., Galea, M. P., Hodges, P. W., & Chipchase, L. S. (2012). Primary sensory and motor cortex excitability are co-modulated in response to peripheral electrical nerve stimulation. *PLoS ONE*, *7*, e51298. <https://doi.org/10.1371/journal.pone.0051298>
- Schoffelen, J., & Gross, J. (2009). Source connectivity analysis with MEG and EEG. *Human Brain Mapping*, *30*, 1857–1865. <https://doi.org/10.1002/hbm.20745>
- Solopchuk, O., Alamia, A., & Zénon, A. (2016). The role of the dorsal premotor cortex in skilled action sequences. *The Journal of Neuroscience*, *36*, 6599–6601. <https://doi.org/10.1523/JNEUROSCI.1199-16.2016>
- Tadel, F., Baillet, S., Mosher, J. C., Pantazis, D., & Leahy, R. M. (2011). Brainstorm: A user-friendly application for MEG/EEG analysis. *Computational Intelligence and Neuroscience*, *2011*, 1–13, 879716. <https://doi.org/10.1155/2011/879716>
- Tadel, F., Bock, E., Niso, G., Mosher, J. C., Cousineau, M., Pantazis, D., Leahy, R. M., & Baillet, S. (2019). MEG/EEG group analysis with brainstorm. *Frontiers in Neuroscience*, *13*, 76. <https://doi.org/10.3389/fnins.2019.00076>
- Tanji, J., & Wise, S. (1981). Submodality distribution in sensorimotor cortex of the unanesthetized monkey [WWW document]. *Journal of Neurophysiology*, *45*, 467–481. <https://doi.org/10.1152/jn.1981.45.3.467>
- Tecchio, F., Zappasodi, F., Pasqualetti, P., & Rossini, P. M. (2005). Neural connectivity in hand sensorimotor brain areas: An evaluation by evoked field morphology. *Human Brain Mapping*, *24*, 99–108. <https://doi.org/10.1002/hbm.20073>
- Torquati, K., Pizzella, V., Della Penna, S., Franciotti, R., Babiloni, C., Rossini, P. M., & Romani, G. L. (2002). Comparison between SI and SII responses as a function of stimulus intensity. *Neuroreport*, *13*, 813–819. <https://doi.org/10.1097/00001756-200205070-00016>
- Tumati, S., Martens, S., de Jong, B. M., & Aleman, A. (2019). Lateral parietal cortex in the generation of behavior: Implications for apathy. *Progress in Neurobiology*, *175*, 20–34. <https://doi.org/10.1016/j.pneurobio.2018.12.003>
- Urasaki, E., Genmoto, T., Akamatsu, N., Wada, S., & Yokota, A. (2002). The effects of stimulus rates on high frequency oscillations of median nerve somatosensory-evoked potentials—Direct recording study from the human cerebral cortex. *Clinical Neurophysiology*, *113*, 1794–1797. [https://doi.org/10.1016/S1388-2457\(02\)00291-2](https://doi.org/10.1016/S1388-2457(02)00291-2)
- Valeriani, M., Le Pera, D., & Tonali, P. (2001). Characterizing somatosensory evoked potential sources with dipole models: Advantages and limitations. *Muscle & Nerve*, *24*, 325–339. [https://doi.org/10.1002/1097-4598\(200103\)24:3<325::AID-MUS1002>3.0.CO;2-0](https://doi.org/10.1002/1097-4598(200103)24:3<325::AID-MUS1002>3.0.CO;2-0)

## SUPPORTING INFORMATION

Additional supporting information can be found online in the Supporting Information section at the end of this article.

**How to cite this article:** Hssain-Khalladi, S., Giron, A., Huneau, C., Gitton, C., Schwartz, D., George, N., Le Van Quyen, M., Marrelec, G., & Marchand-Pauvert, V. (2024). Further characterisation of late somatosensory evoked potentials using electroencephalogram and magnetoencephalogram source imaging. *European Journal of Neuroscience*, *60*(1), 3772–3794. <https://doi.org/10.1111/ejn.16379>